Geochemistry Geophysics Geosystems G3
AN ELECTRONIC JOURNAL OF THE EARTH SCIENCES
Published by AGU and the Geochemical Society

Article
Volume 11, Number 3
6 March 2010
Q03002, doi:10.1029/2009GC002811
ISSN: 1525-2027

Delamination or slab detachment beneath Vrancea? New arguments from local earthquake tomography

Ivan Koulakov
Institute of Petroleum Geology and Geophysics, Novosibirsk 630090, Russia (koulakoviy@ipgg.nsc.ru)

Also at German Research Centre for Geosciences, D-14473 Potsdam, Germany

Bogdan Zaharia
National Institute for Earth Physics, Calugareni str. 12, PO Box MG-2, 077125 Magurele, Romania (bzaharia@infp.ro)

Bogdan Enescu
National Research Institute for Earth Science and Disaster Prevention, Tsukuba 305-0006, Japan

M. Radulian and M. Popa
National Institute for Earth Physics, Calugareni str. 12, PO Box MG-2, 077125 Magurele, Romania (mircea@infp.ro; mihaela@infp.ro)

Stefano Parolai and J. Zschau
German Research Centre for Geosciences, D-14473 Potsdam, Germany

[1] Vrancea, located at the southeastern Carpathians Arc bend, is one of the areas in the Alpine-Himalayan belt that features strong earthquakes occurring at intermediate depths (60–200 km). In this study we investigated the crustal and lithospheric structure beneath the Vrancea seismic area using a local earthquake tomography approach. We used an updated and revised catalog, spanning from 1982 to 2006 that uses data from both permanent and temporary networks in the target area. Simultaneous tomographic inversion for the Vp and Vs anomalies and the Vp/Vs ratio and source locations was done using the LOTOS code. The reliability and robustness of the results were rigorously checked using various tests (e.g., by studying the role of different parameters on the results of the inversion, performing the inversion using random data subsets, and synthetic modeling). The tomography results clearly indicate the presence of a high-velocity material beneath Vrancea at a depth interval of about 60–200 km that coincides with the distribution of intermediate-depth seismicity. This result agrees generally with previous tomographic studies. We compare two scenarios leading to this structure: (1) subduction and slab detachment and (2) ''drop forming'' or delamination. The latter mechanism presumes that the thickening of the crust due to continent-continent collision causes transformation of the mafic lower crust into denser eclogite. This material accumulates until it reaches a critical mass, at which point it forms a large drop that begins to fall down. We propose that the high-velocity anomaly we observe in our tomogram might represent the descending eclogitic lower crust material enveloped by the entrained lithosphere. It is possible that a similar delamination process can be observed in other parts of the Alpine-Himalayan belt, such as in the Pamir Hindu-Kush area.

Components: 11,982 words, 17 figures, 3 tables.

Keywords: seismic tomography; Vrancea (Romania); delamination; slab detachment.

Index Terms: 7270 Seismology: Tomography (6982, 8180); 7218 Seismology: Lithosphere (1236); 8120 Tectonophysics: Dynamics of lithosphere and mantle: general (1213).

Received 27 August 2009; **Revised** 5 November 2009; **Accepted** 9 November 2009; **Published** 6 March 2010.

Koulakov, I., B. Zaharia, B. Enescu, M. Radulian, M. Popa, S. Parolai, and J. Zschau (2010), Delamination or slab detachment beneath Vrancea? New arguments from local earthquake tomography, *Geochem. Geophys. Geosyst.*, *10*, Q03002, doi:10.1029/2009GC002811.

1. Introduction

[2] The interaction of lithospheric plates is one of the most important and intriguing geological processes on Earth. Collisions of ocean-ocean and ocean-continent plates occur through the subduction of the oceanic plates, and their general mechanism is roughly understood and accepted by most scientists. On the contrary, many aspects of continent-continent collisions remain enigmatic. In some continental areas, collisions of continental plates cause considerable surface shortening that may reach several hundred kilometers (e.g., in central Asia due to the India-Asia collision). Many questions related to this topic are actively debated. For example, what happens to the mantle section of the continental lithosphere during the continent shortening? In such cases we usually observe a coupling of the crust, but the lithospheric mantle does not increase in thickness. Why is the stable cratonic-type lithosphere usually thicker than that in the collision belts? Why is the lithosphere in these belts not coupled? What is the mechanism for recycling the mantle continental lithosphere? Does it sink, like the oceanic lithosphere?

[3] In some collisional areas of continental Asia, intermediate-depth seismicity at depths of more than 100 km is observed (e.g., Pamir-Hindu-Kush, Zagros, Burma, and Vrancea). To explain this phenomenon, many authors draw a parallel with classical subduction of oceanic plates, presuming the existence of a sinking oceanic lithosphere in the upper mantle. For the areas of Zagros and Burma located close to oceanic basins, such a mechanism seems plausible. However, for the Pamir Hindu-Kush and Vrancea regions such an explanation is debatable, since there is no clear evidence of oceanic basins existing in these regions in the recent past (e.g., less than 10 MA). In this paper we conduct a local tomography study for the Vrancea region and based on our results, we try to find out which mechanism is most probable for the Vrancea region. The conclusions made in this case may be generalized for explaining the mechanisms of lithosphere recycling also in other cases of continent-continent collision.

[4] Understanding the nature of tectonic processes that take place in the highly populated areas of the Alpine mountain system is also important for mitigating seismic risk in the region. The most intriguing feature of the Vrancea region is the very active intermediate-depth seismicity, densely concentrated in a vertically oriented cluster below a depth of 60 km. Strong earthquakes ($M > 7.0$) that can produce significant damage over large areas occur periodically in this deep cluster (there are roughly 2–3 earthquakes per century). Although many different multidisciplinary geological and geophysical studies have been performed in the Vrancea region, the nature of the intermediate-depth seismicity cluster is still actively debated. In section 2 we will present the important current concepts and ideas that are proposed to explain the occurrence of Vrancea earthquakes.

[5] As will be shown in section 2, the deep structure beneath the Vrancea region has been previously studied by many authors. At the same time we claim that in the present work we have achieved a certain progress in respect to previous studies. First of all, in this study, we used a newly updated local earthquake data set with higher amount and quality of picks than in previous studies. This allowed for a more refined image of the underground structure in the Vrancea region. Second, we used a code for tomographic inversion and source location, LOTOS [*Koulakov*, 2009], which has some particular features not present in the codes used in previous studies (see section 3). We verified the results by performing many different robustness and synthetic tests (see Appendices A–E). They were also used to evaluate the optimal values of the free parameters used in the inversion and estimate the spatial resolution of the resulting model.

[6] It is worth noting that seismic tomography still remains an imperfect tool, and different authors often provide noncoherent images for the same

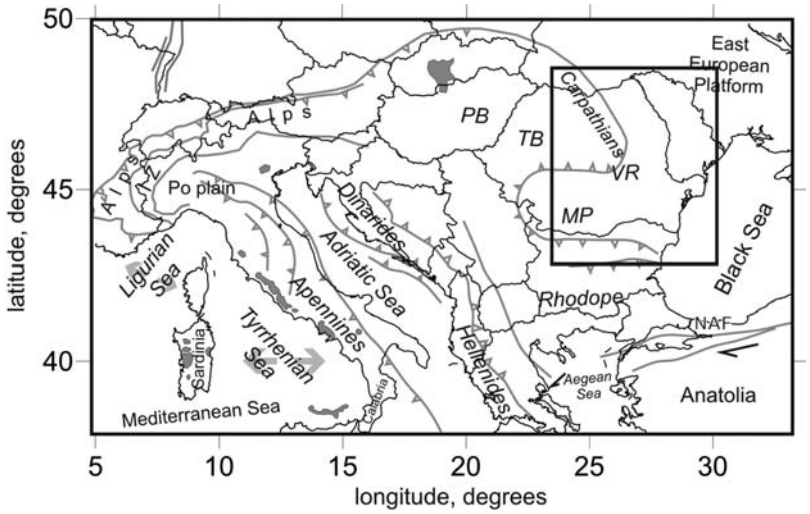

Figure 1. Main tectonic elements in Carpathian-Mediterranean region. The rectangle marks the area of interest for this study. Abbreviations are as follows: IZ, Ivrea Zone; MP, Moesian Platform; NAF, North Anatolian Fault; PB, Pannonian Basin; TB, Transylvania Basin; VR, Vrancea.

areas and even for the same data sets. Thus, performing independent inversions based on independent algorithms and data helps to identify the most robust results and provides important information for the validation of different seismotectonic models.

2. Geotectonic Setting of the Area and Previous Seismic Studies

[7] The Vrancea region is part of the Carpathian mountain system, which, in turn, represents a northeastern branch of the Alpine fold-and-thrust system (Figure 1). The tectonic development of the Alpine system began in the Jurassic and is mostly controlled by the collision of three large continental plates: the Eurasian, African, and Arabian. This collision caused the formation of extremely complex tectonic structures, consisting of many microplates and folded belts. The Carpathian orogenesis appears to be due to the shaping of the boundary of the East European Platform, which forms a loop in the Vrancea region (Figure 2). The southeastern Carpathian Arc bend is located at the confluence of three main tectonic units (east European plate, IntraAlpine subplate and Moesian subplate) in the Vrancea region of Romania (Figure 1). The collision of this segment of the Alpine belt began in the Cenozoic as a result of the lateral eastward extrusion caused by the continuous convergence in Alps [*Ratschbacher et al.*, 1991]. In the Vrancea region, an oceanic basin, floored by an oceanic crust, lays in the area of the present-day Carpathians which was consumed by subduction during Tertiary times [*Burchfiel*, 1976; *Csontos*, 1995; *Csontos and Voros*, 2004]. A total width of 130 km of the basin was subducted during the first episode, with a convergence rate of approximately 2.5 cm yr^{-1} [*Roure et al.*, 1993; *Roca et al.*, 1995]. The active shortening process stopped during the late Oligocene–Early Miocene periods (about 20 MA) when all the oceanic-type basins were closed [*Ellouz and Roca*, 1994; *Linzer et al.*, 1998].

[8] In contrast with the eastern Carpathian branch, where the convergence of the plates seems to be currently inactive, complex active processes still take place beneath Vrancea in a very confined area. The brightest manifestation of this process is a cluster of intermediate seismicity beneath Vrancea in a narrow nearly vertical volume at depths below 60 km, which is clustered along a NE–SW direction [e.g., *Wenzel et al.*, 1999; *Radulian et al.*, 2008; *Radulian and Popa*, 1996]. Large intermediate-depth events with magnitude M = 6.5 occur two to five times per century. During the last century there were four large events: in 1940 (M = 7.7), in 1977 (M = 7.5), in 1986 (M = 7.2) and in 1990 (M = 6.9) which caused serious damages in the neighboring areas. The shallow seismicity in this area is much weaker.

[9] Several seismic tomography studies have been previously performed in this region. The first studies investigating the three-dimensional velocity structure in the Vrancea area used the P wave arrivals from teleseismic earthquakes recorded by

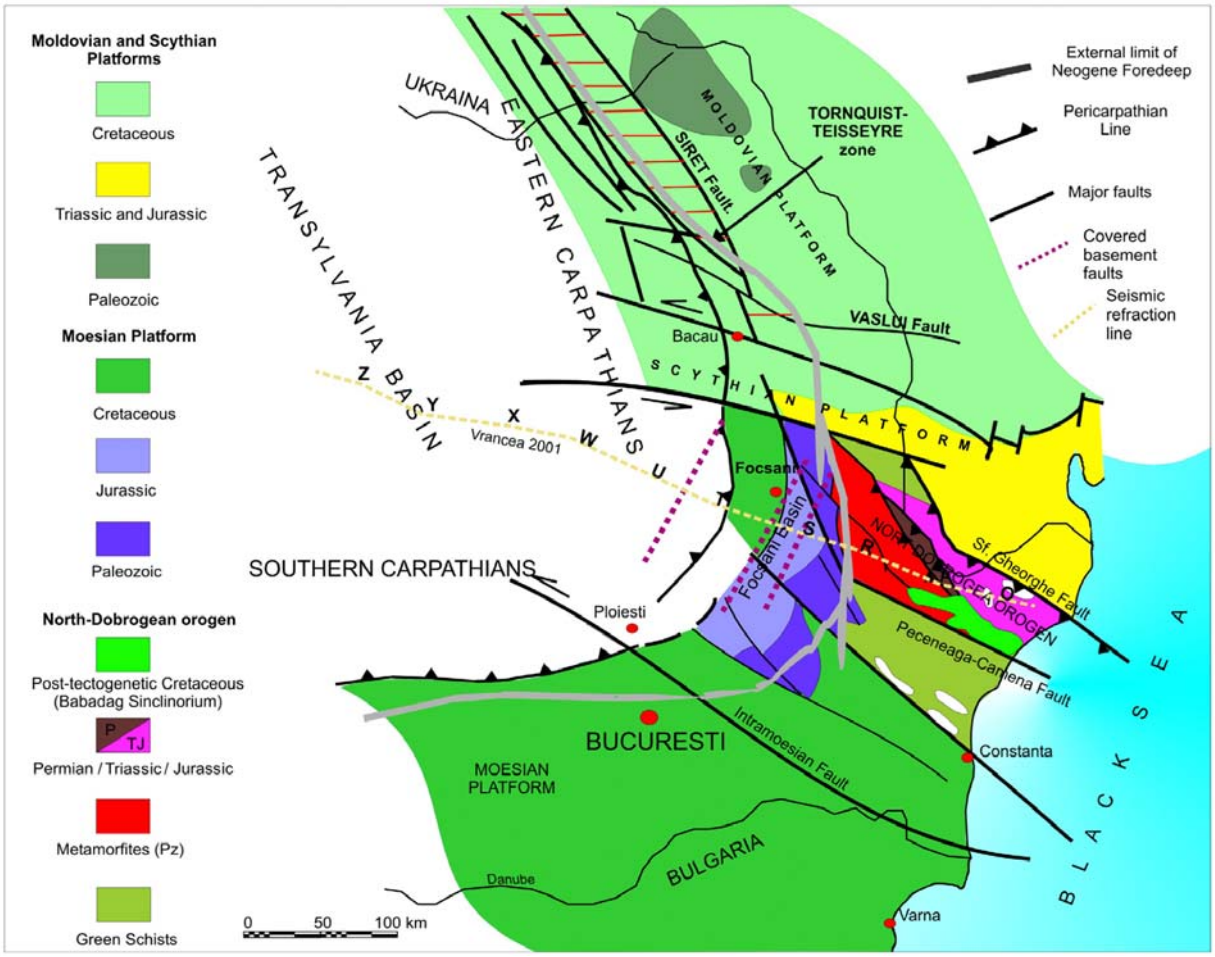

Figure 2. Southeastern Carpathian arc bend tectonic map (modified after *Badescu* [2005]).

the Romanian Seismic Network [*Fuchs et al.*, 1979; *Oncescu*, 1982, 1984; *Oncescu et al.*, 1984; *Koch*, 1985]. Later studies [*Wortel and Spakman*, 1992; *Lorenz et al.*, 1997; *Fan et al.*, 1998; *Popa et al.*, 2001] inverted for the velocity structure using P and S phase arrivals and attenuation [*Popa et al.*, 2005] from local and regional events. Significant advances in the understanding of the deep seismic structure and seismicity in the Vrancea region were achieved as a result of the CALIXTO'99 experiment [*Wenzel et al.*, 1998]. In particular, important results about the 3-D velocity structure in the mantle beneath the Vrancea area were obtained by *Martin et al.* [2005, 2006] from inversion of teleseismic data recorded within this experiment.

[10] The aforementioned tomographic studies based on local, regional and teleseismic earthquake data put into evidence the high-velocity body located between 60 and 200 km depth, which sinks into the asthenosphere almost vertically. This velocity pattern can be observed in the region where the Vrancea subcrustal seismic activity occurs. Studies of conversion waves coming from earthquakes that occurred in the Vrancea region and recorded at seismic stations in Romania [e.g., *Enescu et al.*, 1982] also suggest the presence of a quasi-vertical lithosphere fragment, located between depths of about 80 to 200 km. The teleseismic tomography by *Martin et al.* [2005] also evidenced a change in the orientation of the high-velocity body, from a NE–SW direction in the upper part to a N–S direction in the lower part. The P wave velocity anomalies in this pattern are estimated to be at about 3% with respect to the 1-D reference model. Above this high-velocity anomaly, the tomography results reveal the existence of a low-velocity structure. These findings have also been supported by analysis of seismic attenuation along rays from deep events beneath Vrancea performed by *Russo et al.* [2005].

[11] The occurrence of the intermediate-depth seismicity within the high seismic velocities in the upper mantle is interpreted as the transportation of

cold and dense lithospheric material into the upper mantle. However, one major question that arises when trying to explain this process concerns the type of the descending material: is it a subducted oceanic lithosphere fragment or a delaminated continental material?

[12] Early geodynamical models [e.g., *McKenzie*, 1970] suggested that the intermediate-depth earthquakes beneath Romania occur in a relic oceanic slab sinking vertically within the mantle beneath the continental crust. Based on the existence of a gap in seismicity at a depth of 40–60 km [*Fuchs et al.*, 1979; *Constantinescu and Enescu*, 1984; *Oncescu*, 1984] and on the shape of seismic anomalies in aforementioned tomographic studies, many authors propose a mechanism of slab detachment beneath Vrancea. However, given the hypothesis of a complete detachment, it is hard to explain the relatively high strain rates inside the slab (probably associated with the strong slab pull forces). Moreover, a complete decoupling is not compatible with the gravitational instability mechanism. Therefore, a progressive decoupling along the Carpathian arc is proposed by some authors [e.g., *Wortel and Spakman*, 1993; *Matenco et al.*, 1997; *Sperner et al.*, 2001]. One of the strongest arguments in favor of subduction of an oceanic slab beneath the eastern Carpathians is the presence of a linear arc of Neogene volcanism within the hinterland [e.g., *Seghedi et al.*, 2004]. This volcanic chain, which is composed of both calc-alkaline and alkaline magmas, was active from the Middle Miocene to Quaternary time (13.4–0.2 Myr), and migrated successively from north to south [*Mason et al.*, 1998], even though major and trace element geochemistry of the calc-alkaline lavas suggest they are subduction-related [e.g., *Pecskay et al.*, 1995; *Mason et al.*, 1998; *Seghedi et al.*, 2004].

[13] Delamination is one of alternatives to subduction mechanism of the lithosphere "recycling." This mechanism has been used for explaining the geodynamical processes in different areas after classical work on continental lithosphere sinking beneath the Colorado plateau by *Bird* [1979]. Delamination mechanism seems to be suitable for some cases of continent-continent collision [e.g., *Nelson*, 1991; *Houseman and Molnar*, 1997; *Ducea and Saleeby*, 1998; *Gilbert et al.*, 2007] and, particularly, for the Vrancea region [e.g., *Knapp et al.*, 2005]. It may also explain occurrence of mantle seismicity, as, for example, shown by *Seber et al.* [1996] for the area of Alboran Sea. Delamination presumes a periodical localization of denser lithosphere material until it reaches a critical mass, at which point it forms a large drop that begins to fall down. For the Vrancea region, *Lorinczi and Houseman* [2009] have recently modeled the Rayleigh-Taylor gravity instability due to higher density in the lithosphere in respect to the asthenosphere. They obtained a downgoing drop of the lithosphere material and estimated the strain rates caused by this process which appear to be consistent with the focal mechanisms of the intermediate seismicity beneath Vrancea. *Kay and Kay* [1993] have proposed that the delamination process can be triggered by eclogitization of the lower crust material. *Sobolev et al.* [2006] and *Babeyko et al.* [2006] have modeled this situation for a collision area in the central Andes. They have shown that coupling of the continental crust in the collision areas may cause eclogitization of the lowermost crust, that results at accumulation of anomalously high density material in the bottom of the crust. This increases the gravity instability and favors forming falling "drops."

[14] After presenting our tomographic results, in section 5 we will compare the subduction and delamination mechanisms for the Vrancea region in the light of the new findings.

3. Data and Method of Analysis

3.1. Data Description

[15] The earthquake data were provided by the CALIXTO'99 experiment and K2 network within the CRC461 program of University of Karlsruhe (Germany) [*Wenzel et al.*, 1998; *Bonjer et al.*, 2000; *Bonjer and Rizescu*, 2000; *Bonjer et al.*, 2002] and Romanian Seismic Network [*Neagoe and Ionescu*, 2009]. The data set consists of P and S wave arrival times of 994 local events (Figure 3a) that were recorded from 1982 to 2006. The earthquakes were selected by requiring a minimum of six P wave arrivals with a clear onset per event, and an RMS smaller than 0.5 s. There are 687 intermediate-depth events and 307 crustal events that fulfilled this criterion. The distribution of temporary and permanent seismic stations that recorded the earthquakes is shown in Figure 3b. The temporary network was in use during the CALIXTO'99 experiment and consisted of 30 broadband and 90 short-period stations, installed in a region of about 350 km in diameter and centered in the Vrancea area. There were 160 local events (ML = 2.0) that were recorded in a period of six months during CALIXTO'99. In 2006, the Romanian Seismic

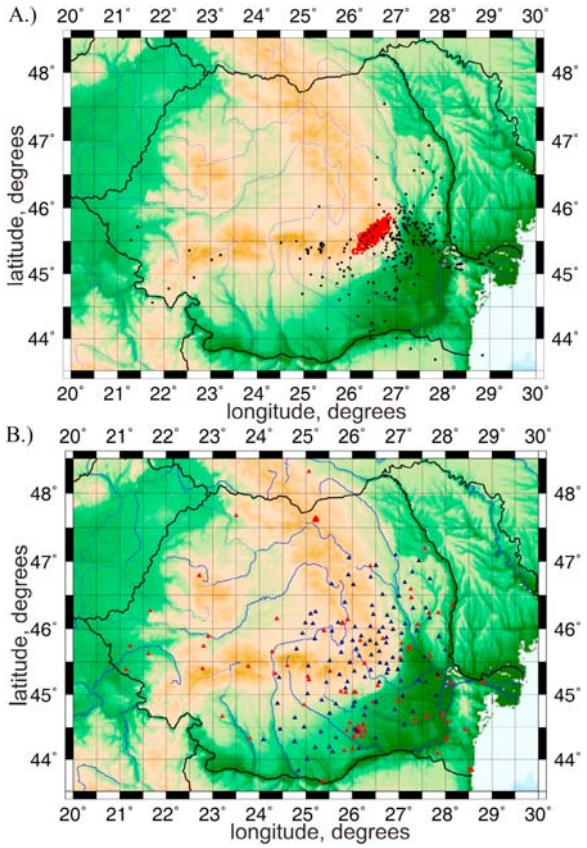

Figure 3. Data used in this study. (a) Earthquake distribution. Red and black dots show intermediate-depth and crustal events, respectively. (b) Seismic stations: blue for temporary network from CALIXTO and red for stations which are sending data to RO-NDC.

Network had about 120 stations in the area between 43.5 and 48°N latitude and 21–29°E longitude. Most of the stations are located in the eastern and southern Carpathians and are primarily designed to survey the Vrancea seismic region, at the Carpathians Arc Bend. The initial event locations were found using the HYPOPLUS program [*Oncescu et al.*, 1996], which is used by NIEP for routine earthquake locations [*Oncescu et al.*, 1999]. The quality of the initial earthquake locations is relatively high, with a mean value of RMS travel time residuals below 0.5 s. To select data for the tomographic inversion we performed additional analysis to reject the outliers and events with less than 10 picks. The final data set consists of 16199 arrival times from 653 events with 8529 P wave and 7670 S wave arrival times.

3.2. Inversion Method

[16] The 3-D tomography inversion was performed using the LOTOS code which is freely available at http://www.ivan-art.com/science/LOTOS. The code is described in detail by *Koulakov* [2009]. Here we present very briefly the main steps of the algorithm.

[17] The input files for our calculations include the list of the stations with coordinates and elevations, and a catalog of the arrival times from local earthquakes. The algorithm does not require any information about coordinates and origin times of the sources. However, using the preliminary locations of sources allows us to speed up the calculations. In addition, a starting 1-D velocity model and a set of free parameters for different calculation steps should be defined.

[18] The calculation begins with preliminary earthquake locations in a 1-D velocity model. At this stage, the source coordinates and origin times are determined using a grid search method [*Koulakov and Sobolev*, 2006a]. The method ascertains the maximum of a Goal Function (GF) that reflects the probability of the source location in the 3-D space. The model travel times are computed using tabulated values calculated in the 1-D velocity model at a preliminary stage. This makes the preliminary location step relatively fast and stable. The location of sources in the 1-D model alternates iteratively with the optimization step for the 1-D model, which is based on matrix inversion for the 1-D velocities (Vp(z), Vs(z)), source coordinates and origin times.

[19] After performing the preliminary locations and optimization for the 1-D model, the main stage of the tomographic inversion begins. It consists of several steps that are performed sequentially and looped iteratively. In the first step, the sources are relocated in the 3-D velocity model. The rays are traced using the bending method [*Koulakov*, 2009]. In the first iteration, the relocation is performed in the 1-D model, and in the following iterations it uses previously updated 3-D models. The second step is parameterization grid construction. The LOTOS-09 code gives two possibilities for the parameterization: with cells and with nodes. Here we use only the node parameterization, which we found to be more robust. The main feature of the parameterization in the LOTOS code is the minimization of any effect of grid configuration upon the result. This is achieved by reducing the node spacing to values that we assume to be significantly smaller than the expected size of anomalies. Furthermore, we reduce the bias of the chosen grid configuration on the final tomographic images by repeating the inversion using grids with different

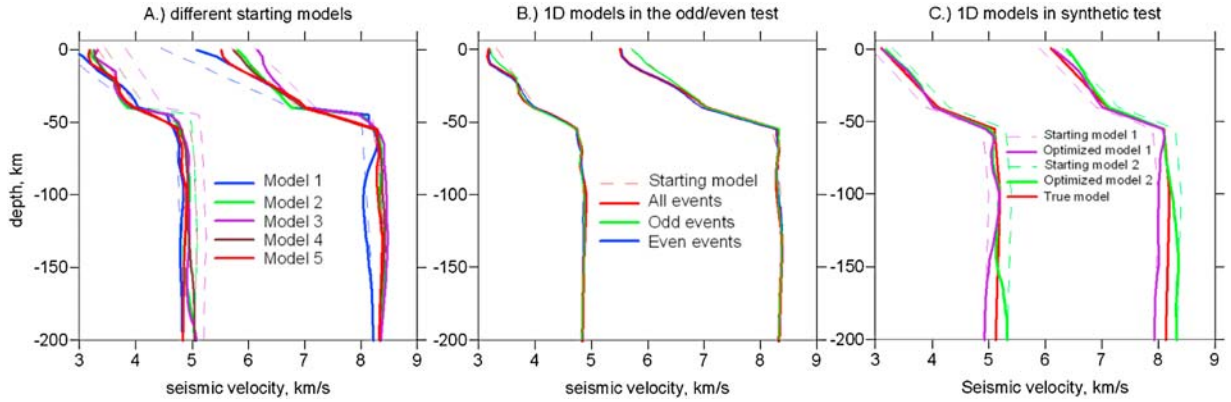

Figure 4. Optimization of the 1-D model for observed and synthetic data. (a) Optimization results with observed data and different starting 1-D models. Different colors indicate different models, dotted lines are the starting models, and bold lines of corresponding colors are the optimization results. (b) Optimization results for halved data subsets in the odd/even test. (c) Optimization results for synthetic data in the checkerboard test presented in Appendix D.

basic orientations (e.g., 0°, 22°, 45°, and 67°) and averaging the results. The matrix inversion for P and S velocity and source parameters (dx, dy, dz and dt for each source) is performed using the LSQR method [*Paige and Saunders*, 1982; *Van der Sluis and van der Vorst*, 1987]. The inversion can also be performed for P velocity and the Vp/Vs ratio using the algorithm described in *Koulakov et al.* [2007]. The amplitude and smoothness of the solution are controlled by two additional matrix blocks. The weights of these blocks play an important role in tuning the resulting model. These parameters, as well as weights for source corrections and other free parameters, are estimated using synthetic modeling.

4. Results

4.1. One-Dimensional Model Optimization

[20] Data processing started with preliminary source location and optimization for the 1-D velocity model. To assess the robustness of this procedure, we performed a series of tests (Figure 4) using the observed and synthetic data. The 1-D model that best explains the observed data was determined using different starting velocity models (Figure 4a). We experimented with different velocities and velocity gradients above and below Moho and used different thickness values for the high gradient layer, which represents the transition from the lower crust to the upper mantle. As an example, some of them are shown in Figure 4a by dotted lines. The RMS values of residuals for five models after their 1-D optimizations are presented in Table 1. All models have significantly different starting values for P and S wave velocity in the crust. The resulting velocity distributions are closer to each other (especially for the S model); however for the P model the difference remains quite significant. Regarding the results related to the mantle, it is shown that the P velocity solution is less robust than that of the S velocity. In fact, for model 1, the resulting distribution of P velocity concurs with the results obtained for other starting models only in the uppermost mantle depth (50–70 km depth). For the deeper layers the result remains close to the starting value. For the S model, the optimization provides similar results for significantly different starting models. It is surprising that for the S wave velocity model the solution appears to be more robust than for the P wave model.

[21] Based on the analysis of the resulting velocity distributions and the RMS of residuals, we can conclude that the most probable 1-D velocity distribution in the Vrancea region corresponds to model 5, which is presented in Table 2. According to this model, the P and S velocities in the mantle are about 8.2–8.3 km/s and 4.8–4.9 km/s, respectively. These values are significantly higher than those used for routine locations of earthquakes in

Table 1. Values of the RMS After Optimization for the 1-D Velocity Distribution With Different Starting Models

Starting Model	RMS of Residuals (s)
Model 1	0.5339
Model 2	0.5131
Model 3	0.5021
Model 4	0.4988
Model 5	0.4968

Table 2. P and S Velocities in the Reference 1-D Model After Optimization[a]

Depth (km)	Vp (km/s)	Vs (km/s)
0	5.51	3.18
10	5.68	3.20
20	6.18	3.63
30	6.67	3.72
40	7.02	3.98
50	7.89	4.54
60	8.29	4.76
70	8.32	4.83
90	8.28	4.86
110	8.32	4.90
130	8.38	4.88
150	8.37	4.86
170	8.34	4.85
190	8.33	4.84
210	8.32	4.83
220	8.31	4.83

[a] Model 5.

this area (7.94–8.17 km/s and 3.86–4.58 km/s for P and S models, respectively) and are closer to the values of the minimum 1-D model determined using the VELEST inversion algorithm [*Kissling et al.*, 1994; *Popa et al.*, 2001].

[22] The stability of the solution in the presence of random noise affecting the observed data was assessed by using the "odd/even" event test [e.g., *Koulakov et al.*, 2007]. The test consists of carrying out independent inversions of two randomly selected data subsets (obtained, for example, by selecting from the whole earthquake data set the odd and even numbers of events in the database). The results of the 3-D inversions for this test are presented in Appendix B. Here, we show the optimization results for the 1-D velocity models (Figure 4b). The starting models for the subsets with odd and even events, and for the entire data set, are the same and correspond to model 5 in Figure 4a. It is shown in Figure 4b that the optimization results in all cases are similar. Only for the crustal layers, where slightly higher velocities are derived for the odd data subset, are differences found. This test shows that the chosen set of data does not affect significantly the stability of the 1-D model optimization.

[23] The stability and robustness of the 1-D velocity optimization was also investigated using synthetic modeling. In Figure 4c, we present the optimization results for the checkerboard test. The 3-D reconstruction of the checkerboard model will be discussed in section 4.5. Here, we show the 1-D optimization results based on two presumably incorrect starting velocity distributions. In the first case, the starting P and S velocities (violet lines) are lower than the "true" ones (red lines) by a constant value of 0.2 km/s. In the second case (green lines), the velocities are regularly higher by the same value. It is shown that for the crustal depth the optimizations provide values that are close to the "true" ones, while, for the lower part of the model, the velocity does not deviate from the starting values. This can be attributed to the fact that the majority of the sources are deep and the trade-off between focal depth, origin time and seismic velocities prevents us from obtaining stable solutions for absolute velocities. Again, as in the cases of measured data inversions, for the synthetic reconstructions we observe better stability for the S velocity optimization. It is important to note that in these two checkerboard analysis the RMS of residuals after optimization have similar values: 0.5005 s and 0.4988 s. The fact that considerable velocity variations cause very small changes of RMS explains the rather low stability for absolute velocity determination in this case. At the same time, it will be shown later that the relative 3-D anomalies, which are based on different reference models, are reconstructed similarly. This shows a higher stability of relative anomaly determinations when compared to absolute values in this observation scheme.

4.2. Three-Dimensional Tomographic Inversion

[24] The LOTOS code allows us to perform the inversion in two schemes: for the Vp-Vs and Vp-Vp/Vs ratio. Performing the inversion for both schemes provides additional constraints for the relationship between the amplitudes of P and S anomalies. Note that in the former scheme we minimize the P and S residuals, while in the latter scheme we process the P and P-S differential residuals. This means that the solutions obtained for the S model using the two schemes are independent, which provides additional information to verify the robustness of our results. In this section, we present the 3-D velocity results using Vp-Vs inversion scheme which were selected as the main result of this study. The inversion results for Vp-Vp/Vs scheme are presented in Appendix A. They include Vp, Vs anomalies and Vp/Vs ratio in horizontal and vertical sections (Figures A1–A3). Comparing the results derived independently using these two schemes provides a possibility to assess the robustness of the reported patterns.

Table 3. Values of RMS of P and S Residuals in First and Fifth Iterations in Cases of Different Starting Models and Inversion Schemes

Model Description	RMS of P Residuals, One Iteration (s)	RMS of S Residuals, One Iteration (s)	RMS of P Residuals, Five Iterations (s)	RMS of S Residuals, Five Iterations (s)
Ref model 5, Vp-Vs scheme	0.3637	0.6214	0.2037	0.3301
Ref model 1, Vp-Vs scheme	0.3686	0.6278	0.2113	0.3362
Ref model 5, Vp-Vp/Vs scheme	0.3637	0.6214	0.2090	0.3672

[25] In all cases the inversion was performed in five iterations, which was a compromise between calculation time and the quality of the solution (reducing the nonlinear effect). Increasing the number of iterations would roughly be equivalent to decreasing the damping for an unchanged number of iterations. The RMS of residuals after the 1st and 5th iterations are shown in Table 3. In general, the Vp-Vp/Vs scheme leads to larger RMS than the Vp-Vs inversion. However, this does not mean that the former scheme provides a worse solution than the latter, when taking into account that the inversion for Vp-Vp/Vs ensures minimization of differential P-S residuals, while Vp-Vs scheme minimizes the P and S residuals that are accounted for in the reported RMS.

[26] Figures 5–7 show the results for P and S anomalies in eight horizontal and two vertical sections that correspond to the Vp-Vs inversion scheme which are the main result of this study. The resulting locations of sources after five iterations of coupled inversion around each section are also shown. These anomalies and their possible interpretation will be discussed in detail in section 5.

[27] Any tomographic inversion guaranties obtaining some results, but just reporting the derived seismic structure without sufficient verification seems to be not adequate. We have performed dozens of different tests with real and synthetic data and some of them are presented in Appendices B–E. It particular, it seems to us very important to explore the effect of starting 1-D model on the resulting velocity anomalies (Appendix B). The results of 1-D model optimization (section 4.1) shows that for some depth interval it does not provide stable solution. Does it affect the results

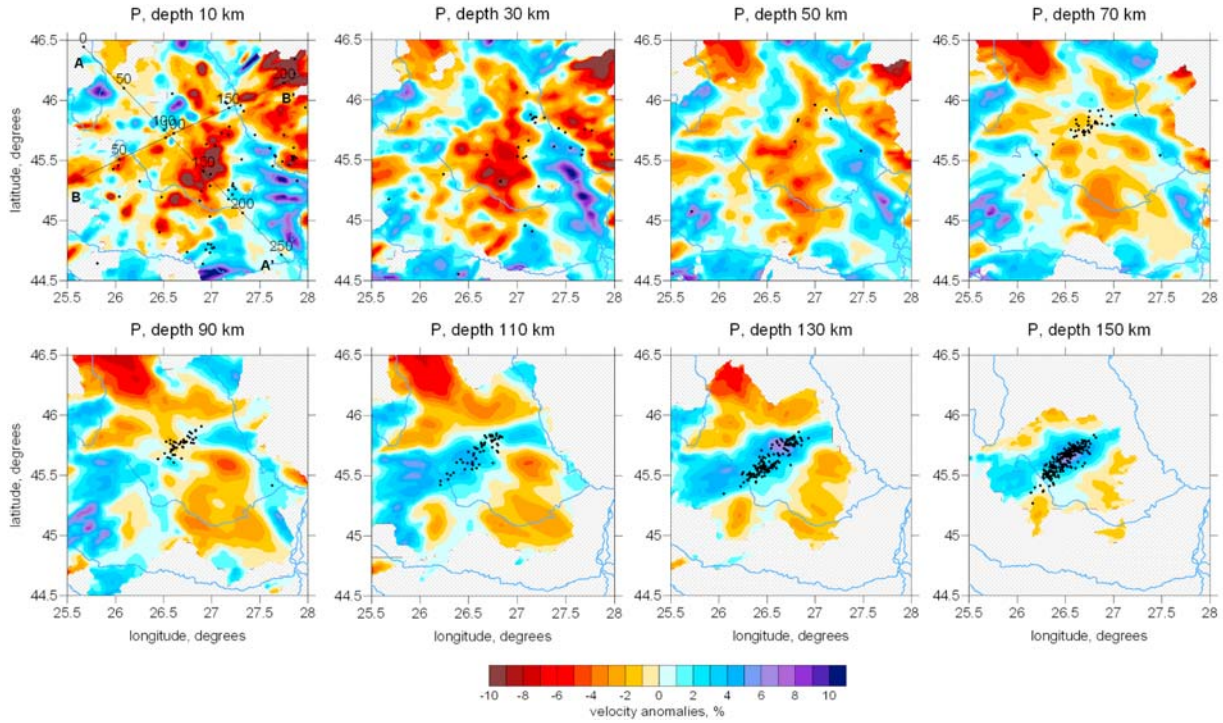

Figure 5. Horizontal sections of P velocity anomalies, in percent with respect to the optimized 1-D velocity model, resulting from the "Vp-Vs" inversion scheme. Dots depict the relocated sources around the corresponding depth levels. Locations of profile presented in Figure 7 are shown in the 10 km depth plot.

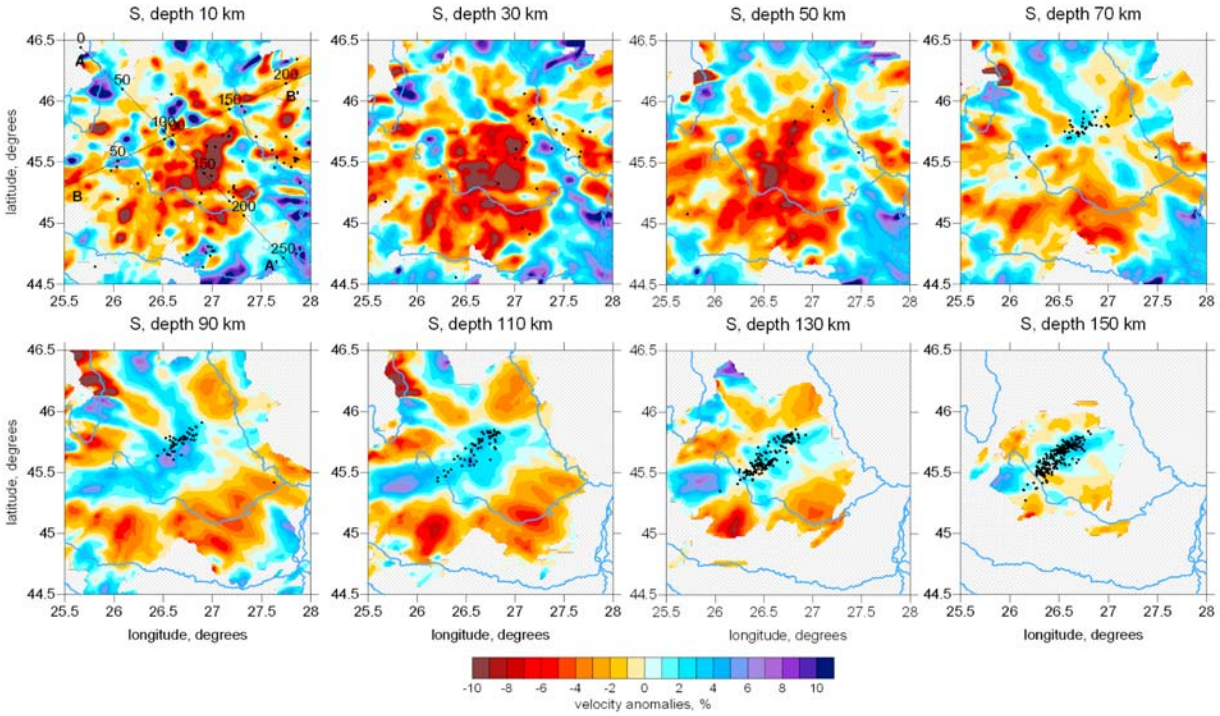

Figure 6. Same as Figure 5 but for the S velocity anomalies.

of 3-D inversion? Comparing the velocity anomalies in the main model (Figures 4 and 5) and ones based on another reference model shows rather good correlation. This means that the reported velocity anomalies appear to be more robust than absolute values. A similar observation has been made by *Koulakov et al.* [2007]. The effect of random noise, which is considerable in the used data set, can be evaluated using independent inversion of two data subset (odd/even test). The results of this test which are discussed in Appendix C reveal the minimal size of trustworthy patterns provided by the existing data set.

[28] In this study we pay much attention to performing synthetic modeling which allows us to find optimal values of free parameters (e.g., damping), to evaluate the spatial resolution, and to estimate the realistic amplitudes of the anomalies. When performing the synthetic tests we simulate as close as possible realistic situations when neither location of sources, nor reference 1-D model are known a priori. In this case the synthetic modeling reveals conservative resolving capacity of tomographic inversion, and it allows us to avoid overinterpreting some questionable anomalies. In Appendix D we describe in details the conditions of performing the synthetic modeling and show the results of 3-D checkerboard test. One of the most important results of this test is that it shows that we have sufficient vertical resolution to distinguish an anomalous body below 65 km depth. Another synthetic test which is presented in Appendix E consists in construction of a model which after consequent performing the forward modeling and inversion enables the same structure as in the case of observed data. If the inversions with identical parameters provide similar models for the cases of real and synthetic data, the synthetic model may adequately represent the velocity distribution in the real Earth. In particular, this test is important to evaluate realistic values of amplitudes of seismic anomalies. Based on a comparison of synthetic and real images we can draw some important conclusions about the amplitudes and shapes of anomalies, which are presented in section 5.

5. Discussion of the Resulting Velocity Patterns and Interpretation

[29] Figures 5–7 show the presence of a high-velocity material in the depth interval of 60 to 180 km, which coincides with the distribution of active intermediate-depth seismicity. These findings generally corroborate the results obtained in previous tomographic studies [*Wortel and Spakman*, 1992; *Lorenz et al.*, 1997; *Martin et al.*, 2005, 2006]. Our results are in qualitative agreement with S velocity model derived from inversion of surface

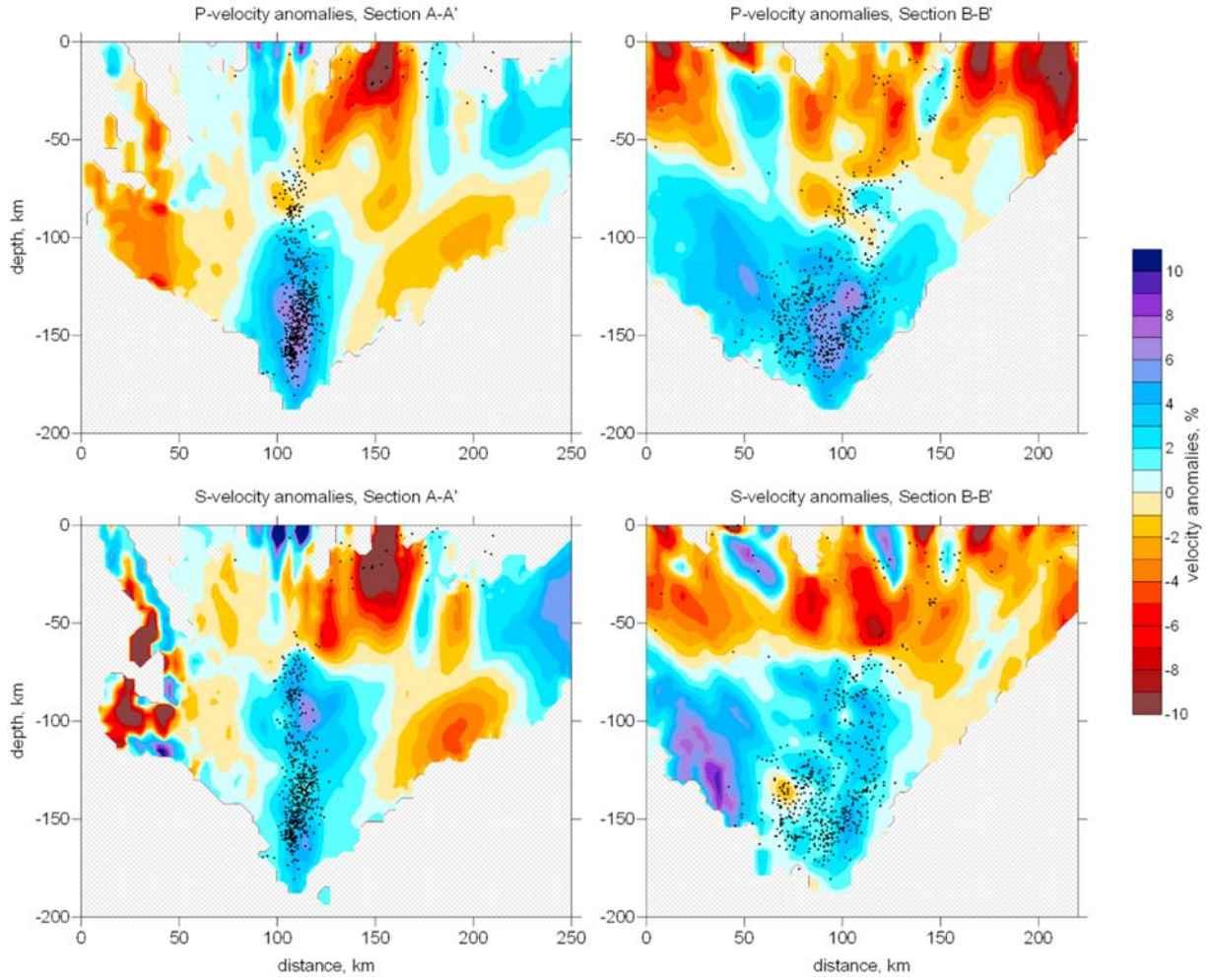

Figure 7. P and S velocity anomalies derived from the "Vp-Vs" inversion scheme in two vertical sections. Locations of the profiles are indicated in Figures 5 and 6. Dots depict the relocated sources at distances of less than 40 km from the profile.

waves by *Boschi et al.* [2009] who found a slow heterogeneity under the Carpathians, underlain by a fast one, with the transition at ~100–150 km depth. The tomography investigations using teleseismic data [*Wortel and Spakman*, 2000; *Martin et al.*, 2006] pointed out a well-defined high-velocity body extending down to a depth of about 400 km. Our results, obtained from the inversion of local data, generally agree with the previous studies, showing, however, a better resolved geometry for the crust and upper mantle down to about 200 km beneath the Vrancea seismic area. The velocity anomalies in the crust are generally negative and continue beneath the Vrancea region down to a depth of around 60 km, where very few seismic events are detected (Figure 7). In our study, higher data quality and many different tests performed allow us to single out the most confident features and to see the processes beneath Vrancea from another point of view. In the following, we consider both the slab detachment and delamination models for the lithosphere recycling beneath Vrancea.

[30] In Figure 8a we present an interpretation cartoon for a subduction and slab detachment scenario beneath the Vrancea region, which is overlapped by our tomographic results in a vertical section. In our tomogram, the deep high-velocity body is clearly separated from the high-velocity Moesian block, which does not agree with the concept of current progressive decoupling [e.g., *Wortel and Spakman*, 1993; *Matenco et al.*, 1997; *Sperner et al.*, 2001]. In the vertical section, we see that the distance between these high-velocity bodies is about 50 km. Seismic activity inside the deep body indicates that it cannot be suspended in a steady state and that it should progressively move

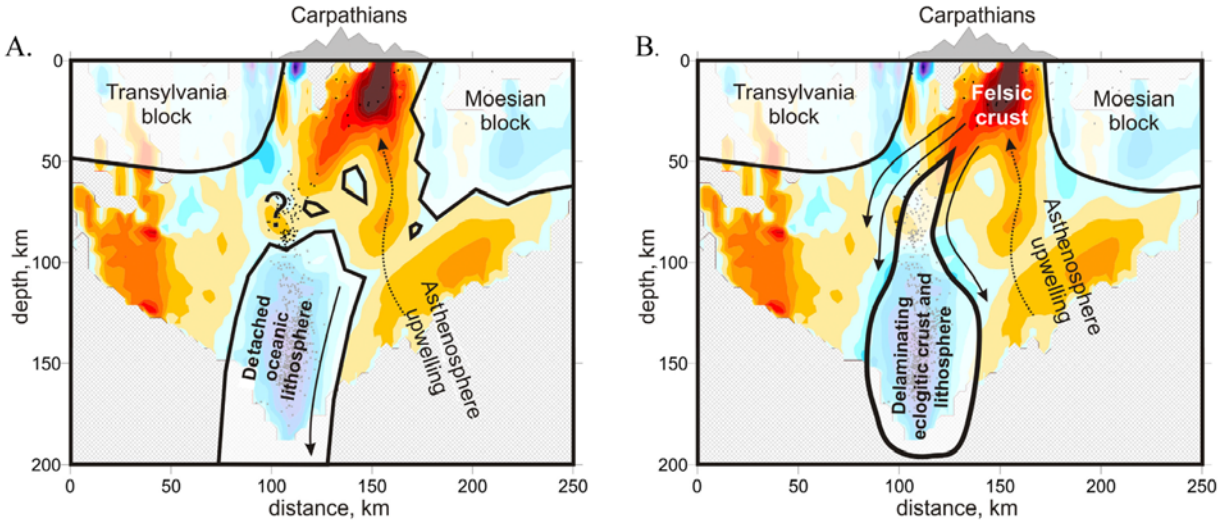

Figure 8. Interpretation cartoons based on the concept of (a) subduction and slab detachment and (b) delamination. Background is the velocity distribution and events resulting from the tomographic inversion (P anomalies, section A–A′), same as in Figure 7.

down. Let us consider an underestimated rate of sinking at 1 cm/year which is much slower than 2.5 cm/yr rate of pre-Oligocene convergence estimated by *Roca et al.* [1995]. With a lower rate, the stresses would probably be too low to produce seismic activity. Dividing the 50 km gap between high-velocity bodies to this rate, we can estimate that the detachment occurred about 5 Ma or less. If we associate this detachment with the closing of an oceanic basin, this brings us logically to a conclusion that before this age in Vrancea area there was an oceanic lithosphere. However, if an ocean-floored basin was consumed during the formation of the eastern Carpathians, evidence for the former boundary between two distinct continental plates should have been recorded in both the surface geology (suture zone) and the underlying crustal structure. To date, no conclusive evidence has been found for such a recent (5 Ma) crustal (and lithospheric) boundary. On the other hand, some authors argue that detachment does not need to occur immediately after subduction stops. For example *van de Zedde and Wortel* [2001] show that due to a rather long transition zone of the lithosphere from the oceanic to continental type, there can be a delay of millions of years. However, according to [*Ellouz and Roca*, 1994; *Linzer et al.*, 1998], active shortening stopped at about 20 MA. It means more than 15 million years of delay between closing of the oceanic basin and detachment of the slab. At the same time, results of numerical modeling usually provide much shorter time of the break-off occurrence [e.g., *Buiter et al.*, 2002]. Furthermore, this explanation presumes that the detached lithosphere is not of oceanic type, but mostly continental. The relatively low density of this detached block prevents fast sinking which is necessary for producing the observed high strain rates.

[31] Detailed comparison of the intermediate-depth seismicity with the shape of the high-velocity body does not corroborate the idea of slab detachment. Indeed, intermediate seismicity in classical oceanic subduction zones is localized close to the upper surface of a slab. In some cases, it can form double seismic zones [e.g., *Nakajima et al.*, 2001], however, both earthquake planes are parallel to the slab upper interface. In the case of Vrancea, the deep seismicity begins at a depth of 60 km where we can still observe low velocity (in area with question mark in Figure 8a). Deeper, the cluster is traced down almost vertically. It passes throughout the central part of the high-velocity "slab," while in the classical subduction model it should be observed closer to the upper (left in the presented section) border of the subducted lithosphere. Furthermore, the large variety of focal mechanism solutions for Vrancea earthquakes and the complexity of the compression and tension axes orientations [e.g., *Enescu and Enescu*, 1998] are also difficult to explain using the framework of classical subduction. Based on the arguments presented in the above paragraphs, we assume that the concept of subduction and slab detachment in the Vrancea case contradicts some of the estimates and observations.

[32] Delamination, as an alternative to subduction mechanism of the lithosphere "recycling" was

initially proposed by *Bird* [1979] and further developed by other authors [e.g., *Kay and Kay*, 1993; *Sobolev et al.*, 2006; *Babeyko et al.*, 2006]. According to some authors, the delamination mechanism is suitable for the cases of the Vrancea region [e.g., *Knapp et al.*, 2005]. A possibility of the two alternative mechanisms, slab detachment and delamination, is also discussed by *Russo et al.* [2005] based on attenuation of seismic waves from deep events beneath Vrancea.

[33] Interpretation of our tomography results in terms of delamination mechanism is presented in Figure 8b. This scenario can be supported by results of *Babeyko et al.* [2006] based on 2-D numerical modeling [*Babeyko et al.*, 2006, Figure 24.4]. In this model, the crust consists of two layers: these are felsic upper and mafic lower crust. At the initial step of compression, the crust is laterally homogeneous and the lithosphere is slightly thinned in the central part of the model. The compression causes maximal deformations in the central part of the model where the lithosphere is weakest [e.g., *Lankreijer et al.*, 1997]. This deformation leads to considerable thickening of the crust (both felsic and mafic layers). Due to the deepening of the mafic material and the changing of the P-T conditions, it is transformed to eclogite, which is much denser than the underlying lithosphere. When a critical mass of the eclogitic lower crust is accumulated, it forms a drop surrounded by unstable lithosphere material that begins to fall. According to estimates presented by *Babeyko et al.* [2006], the sinking velocity of this drop is very high and can reach several dozen centimeters per year. It is obvious that such a high speed can cause abrupt changes in P-T conditions inside the lithospheric drop and very strong stresses that are responsible for the active seismicity. The possibility cannot be excluded that such a fast process leads to phase transitions of the remaining crustal material inside the delaminating drop, which is associated with the release of fluids. In turn, these fluids might decrease the melting temperature of the overlying rocks and may lead to the formation of volcanoes in the area similarly as in the case of oceanic subduction. After delamination, the crust above the falling drop consists mostly of a thick felsic part that can be expected with low seismic velocities. Our tomographic result shows low velocities in the crust beneath Vrancea and seems to corroborate this idea. Also, *Sobolev et al.* [2006] have shown that delamination leads to high topography, which is clearly seen in the Carpathians.

[34] Inferences based on the work of *Babeyko et al.* [2006] must be made with caution, as the modeling exercise conducted by those authors is limited to 2-D, while in the Vrancea area the general structures are 3-D. The natural question when passing from 2-D to 3-D setup is whether these falling material forms in map view isometric "drops" or elongated "walls." Three-dimensional modeling of Rayleigh-Taylor gravity instability [e.g., *Lorinczi and Houseman*, 2009] demonstrates the isometrical character of drops. Intuitively it is clear that elongated "walls" are unlikely. Indeed, in the case of a wet flat ceiling in a bathroom, the drops of water fall more or less chaotically and they are isometric. Even the existence of long beams on the ceiling does not change this feature: the drops are originated as isometric features located at some distances from each other along the beams.

[35] The delamination process and slab detachment seem to be mutually exclusive mechanisms; their combination in the Vrancea region is not likely. The subduction process presumes a continuous penetration of high-velocity material into the mantle, while the delamination mechanism is related to periodic falling of discrete "drops." The time of accumulation of critical mass of the eclogitic material according to the modeling results [*Babeyko et al.*, 2006] is more than ten times longer than that of its falling. We expect that in Vrancea there is a chance to observe a rare process of drop falling, which lasts for a relatively short time when compared to the time of accumulation.

[36] Saying about delamination in Vrancea we should draw parallels with other areas where similar mechanism has been proposed by other authors. Delamination of continental lithosphere is a geodynamic process that has been popular ever since a classic paper on the Colorado Plateau [*Bird*, 1979]. There is a large body of literature on the Sierra Nevada batholith where ongoing aseismic delamination is proposed by *Ducea and Saleeby* [1998], *Gilbert et al.* [2007], and many others. A comprehensive analysis of various data (seismicity, gravity, seismic attenuation and others) for the Alboran Sea in western Mediterranean leads to the conclusion about active delamination of a piece of continental lithosphere [*Seber et al.*, 1996]. Complex interaction of ongoing subduction and delamination of continental Brazilian lithosphere is proposed in the central Andes [e.g., *Kay and Kay*, 1993; *Sobolev et al.*, 2006]. The image of the high-velocity anomaly beneath the Vrancea region is somehow similar to the results obtained

for the Pamir Hindu-Kush region [*Koulakov and Sobolev*, 2006b]. We suppose that a similar delamination mechanism might take place there on a larger scale. In the Pamir Hindu-Kush region, a large high-velocity body in the upper mantle fits with the clusters of very active intermediate-depth seismicity (down to 300 km). This pattern is almost vertical and, in planar view, it is almost isometrical. The seismicity is traced inside this body, not along its border, as presumed in the case of subduction. Furthermore, the subduction concept presumes the sinking of a high-velocity oceanic lithosphere that requires the closing of an oceanic basin in the recent past. However, there is no geological evidence for such a process in the Pamir Hindu-Kush region in the past 50 million years.

[37] We suppose that delamination is one of the main mechanisms of lithosphere recycling in areas of continent-continent collision. In the Alpine-Himalayan belt, the falling of the delaminating drops may occur in any part of the collision zone. However, the time of accumulation of the unstable material is much longer than the time of falling. Therefore, we now have a chance to observe these drops only in two places: in Vrancea and Pamir-Hindu-Kush. Two other areas in Asia where intermediate-depth seismicity can be observed, Zagros (Iran) and Burma, are more likely ascribed to the classical subduction of oceanic plates.

6. Conclusions

[38] The results presented in this study, obtained from the tomographic inversion of local data, generally concur with the results of previous studies, showing however a more highly resolved geometry for the crust and the upper mantle down to about 200 km beneath the Vrancea seismic area. Taking into account the fact that seismic tomography is still an imperfect tool, the observed correlation with the previous results is an informal argument for the robustness of the main patterns derived independently by different authors based on different data sets.

[39] The main resulting feature of the tomographic model derived in this study (as well as in most previous studies) is a high-velocity pattern located below a depth of 60 km, which generally coincides with the distribution of intermediate-depth seismicity. Most of the previous studies interpreted this anomaly as a detached part of an oceanic slab. We present several arguments that contradict this model, such as:

[40] 1. Taking into account the considerable descending speed of this high-velocity "oceanic lithosphere" (at least 1 cm/year), the detachment occurred not earlier than 5 million years ago, which presumes closing of the oceanic basin at the same time. However, there is no evidence of the existence of any oceanic basin in Vrancea in the recent past.

[41] 2. If this body is suspended and does not move down, no seismic activity would be observed in such a steady state system.

[42] 3. The seismicity cluster passes through the central part of the high-velocity body, and is not located close to its upper surface, as presumed by subduction.

[43] We propose an alternative concept of delamination, which can explain most of the existing facts. According to this concept, we currently observe a falling "drop" consisting of eclogitic lower crust material surrounded by untrained lithosphere material. This delamination occurs after a long stage of accumulation of denser eclogitic material in the bottom of the crust. These eclogites are the result of phase transition in the mafic layer due to the thickening of the crust. We propose that this process of accumulation and delamination of eclogitic material might take place in most zones of continent-continent collision. However, the active phase of the falling "drop," which is relatively short compared to the phase of accumulation, is currently observed only in few places (e.g., Hindu-Kush and Vrancea). We hypothesize that delamination, and not subduction, is the main mechanism of recycling the lithosphere material in the continent-continent collisional belts.

Appendix A: Inversion for Vp-Vp/Vs Scheme

[44] Besides the main results which were obtained using the Vp-Vs inversion scheme shown in section 4.2 (Figures 5–7) we present the results computed independently according to Vp-Vp/Vs scheme. The values of the Vp/Vs ratio in horizontal sections derived by inverting the Vp and Vp/Vs ratio are presented in Figure A1. Values of Vp, Vs and Vp/Vs in a vertical section A–A′ are shown in Figure A2. Note that in this case, values of Vs are computed by dividing the resulting Vp by Vp/Vs. Distributions of Vs derived from Vp-Vs and Vp-Vp/Vs schemes are compared in two horizontal sections in Figure A3. The results obtained using the two schemes show similar features for the S

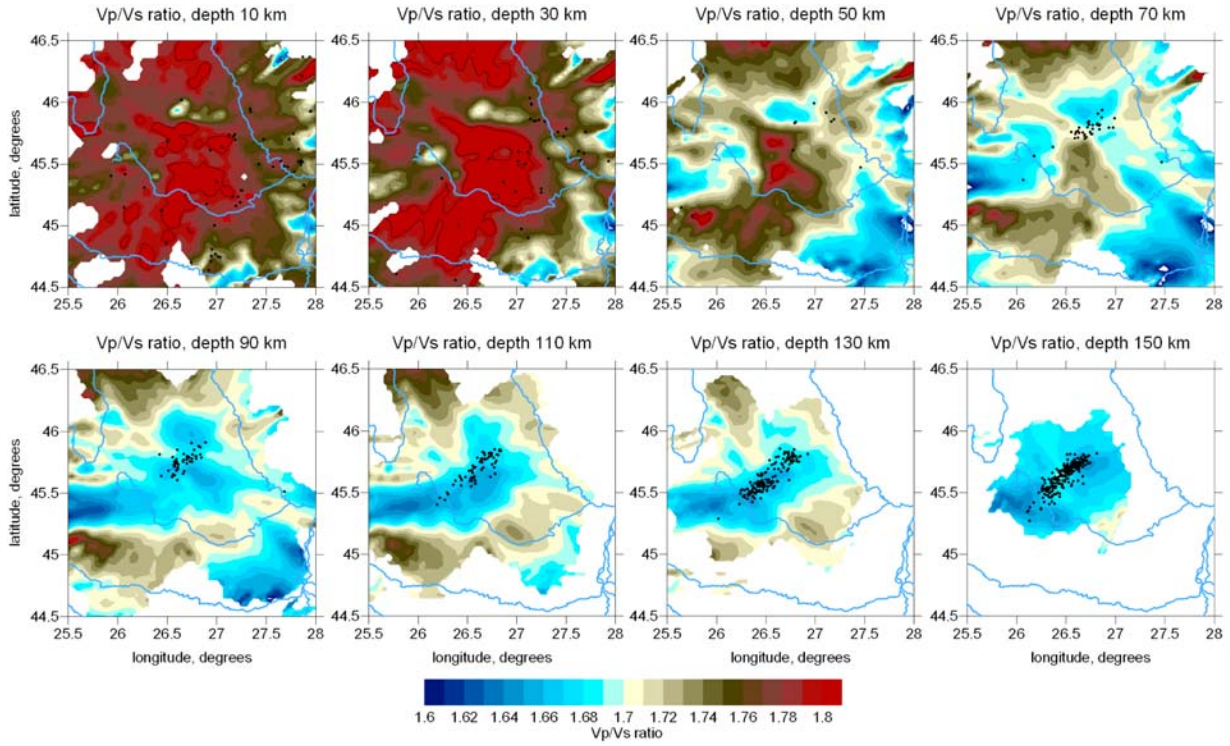

Figure A1. Vp/Vs ratio in horizontal sections derived from the "Vp-Vp/Vs" inversion scheme. Dots depict the relocated sources around the corresponding depth levels.

velocity anomaly, however only at a qualitative level. Although we performed calculations for a dozen sets of free parameters (amplitude damping, smoothing and weighting balance between Vp and Vp/Vs ratio) in each case, we could not achieve an ideal correlation of the amplitudes and shapes of the anomalies. The difference between the results obtained using the two inversion schemes could be related to fundamental differences in the two approaches, namely, minimizing the P and S residuals and the differential P-S residuals.

Appendix B: Effect of the Starting Velocity Model Upon the Resulting 3-D Velocity Anomalies

[45] In section 4.1 we discussed the problem of the relatively low stability of the 1-D reference model

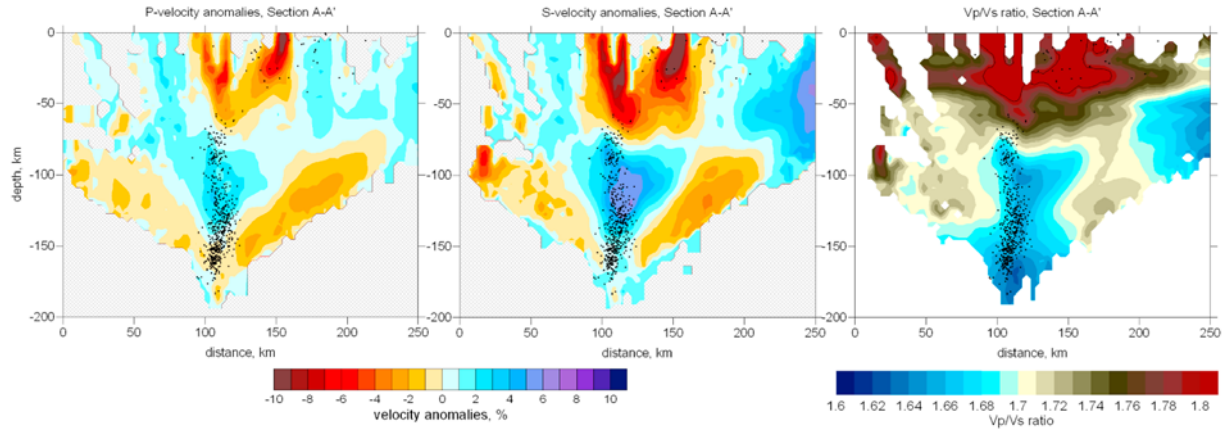

Figure A2. P and S velocity anomalies and Vp/Vs ratio derived from the "Vp-Vp/Vs" inversion scheme in the vertical section A–A′ shown in Figure 5. Dots depict the relocated sources at distances of less than 40 km from the profile.

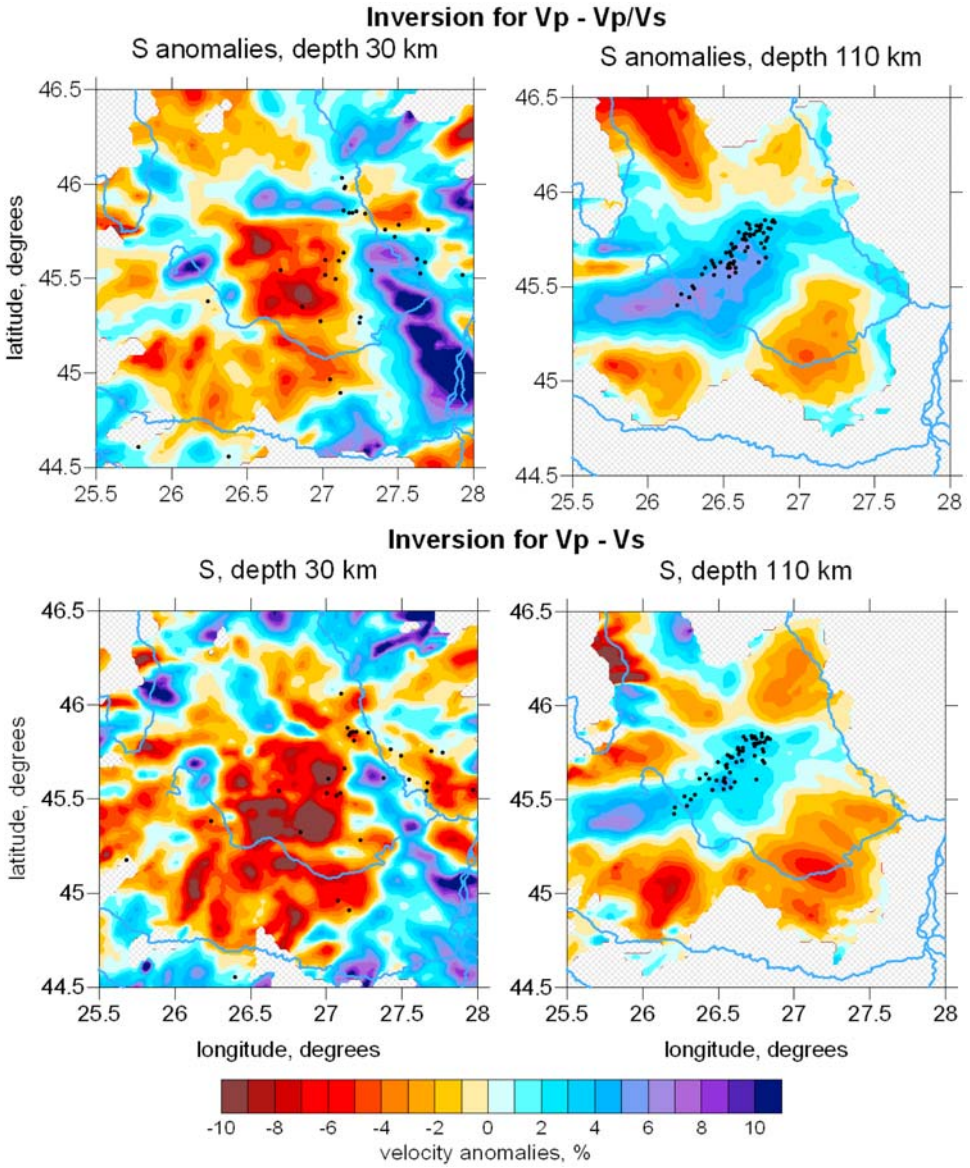

Figure A3. S velocity anomalies obtained using the inversion schemes (top) for Vp-Vp/Vs and (bottom) for Vp-Vs in two horizontal sections. Dots depict the relocated sources around the sections.

optimization. It is important to check how the uncertainty of absolute velocity determination in the starting model for the 3-D inversion affects the relative velocity anomalies. To answer this question, we have performed the full iterative inversion with the same free parameters as for the model presented in Figures 5–7, but based on a different reference model (model 1, blue line in Figure 4a). The resulting patterns in this case, as shown in Figure B1, are almost identical to those in the main model (Figures 5–7), and the RMS value, which is reported in Table 3, is not considerably different. It shows that the relative perturbations are much more robust than the absolute velocity values. A similar observation has been made by *Koulakov et al.* [2007].

Appendix C: Odd/Even Test

[46] Study of the posterior residuals after the inversion shows that the data set used in this study is rather noisy. The contribution of the random noise upon the final result can be estimated using the "odd/even test" (see also section 4.1). The inversion procedure is identical to the one used to derive the major results (Figures 5–7) and includes the step of 1-D model optimization. The resulting 1-D distributions for the odd and even data subsets are

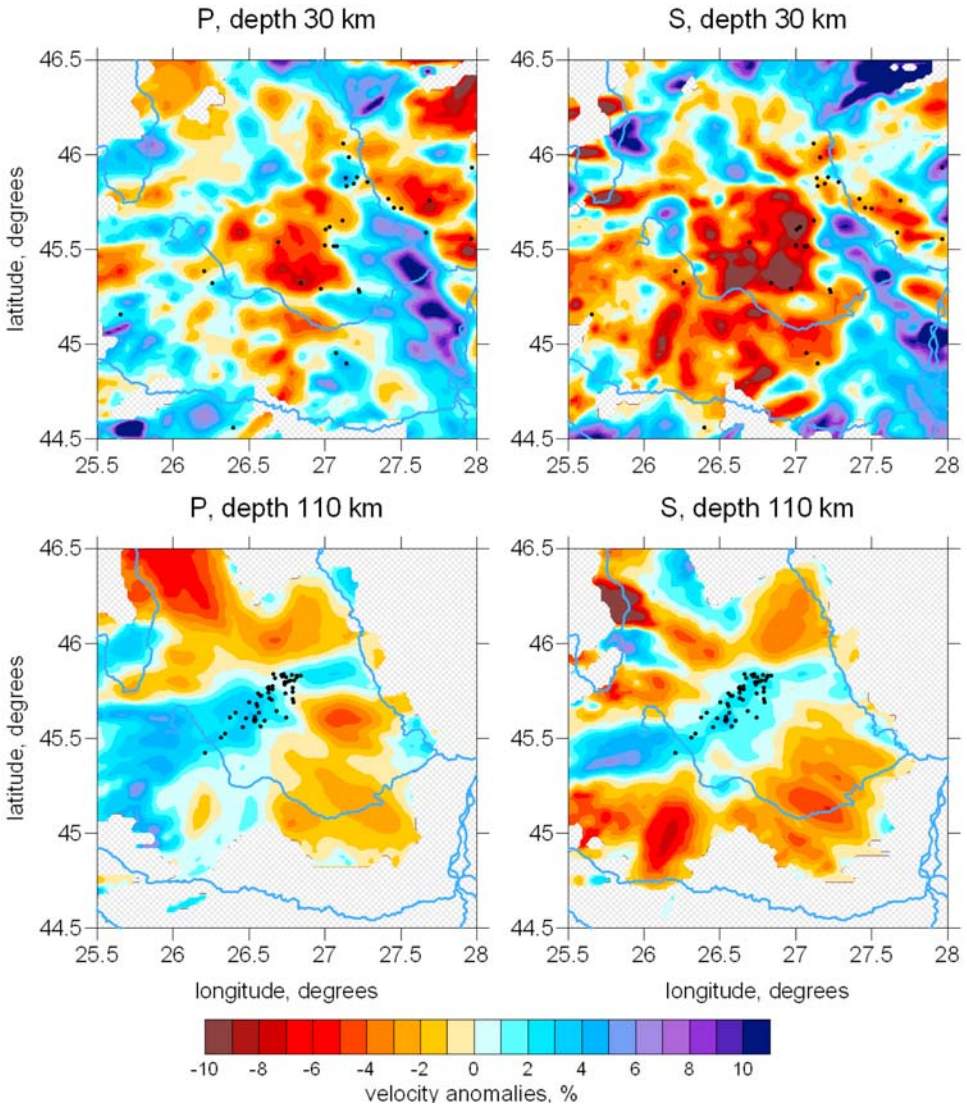

Figure B1. P and S velocity anomalies from Vp-Vs inversion based on another reference model. Dots depict the relocated sources around the sections.

shown in Figure 4b. It can be seen that despite some discrepancies in the models in the crust, for the major parts the curves appear similar. The results of 3-D P and S velocity reconstructions for the two subsets are presented in horizontal and vertical sections in Figures C1 and C2. Looking at these images, one can immediately identify which anomalies are trustworthy and which ones are caused by noise. For example, at a depth of 30 km, the patterns that are smaller than 30 km are probably not robust. At the same time, a large negative anomaly in the central part of the study area seems to be reliable. Most importantly, the positive anomaly patterns in lowest sections seem to be robust in both shape and amplitude. Comparing these test results with the main results presented in section 4.2 shows that halving the data set also has some effect upon the results and makes the solution less stable.

Appendix D: Checkerboard Test

[47] To assess the spatial resolution of the model we performed a synthetic test using the standard checkerboard input model with alternating positive and negative velocity variation patterns. When performing the synthetic modeling, it is important to carry out the simulations in a manner as close as possible to observed data processing. In particular, it is necessary to adhere to several rules:

[48] 1. The parameterization of the synthetic model used for the forward calculation of the travel times should be different from that used during the

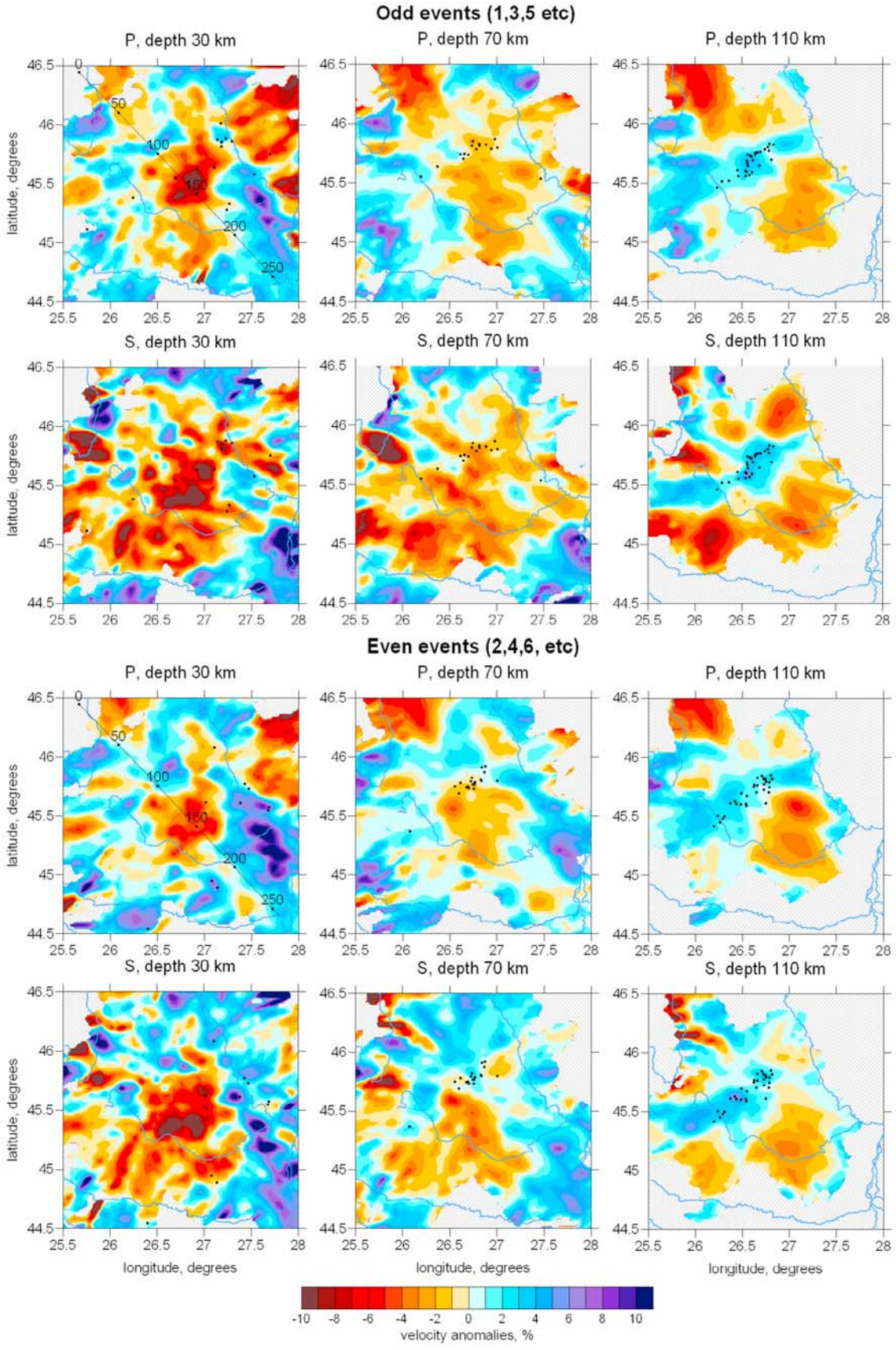
Odd events (1,3,5 etc)
P, depth 30 km
P, depth 70 km
P, depth 110 km
S, depth 30 km
S, depth 70 km
S, depth 110 km
Even events (2,4,6, etc)
P, depth 30 km
P, depth 70 km
P, depth 110 km
S, depth 30 km
S, depth 70 km
S, depth 110 km
latitude, degrees
longitude, degrees
0
50
100
150
200
250
46.5
46
45.5
45
44.5
25.5
26
26.5
27
27.5
28
-10
-8
-6
-4
-2
0
2
4
6
8
10
velocity anomalies, %

Figure C1

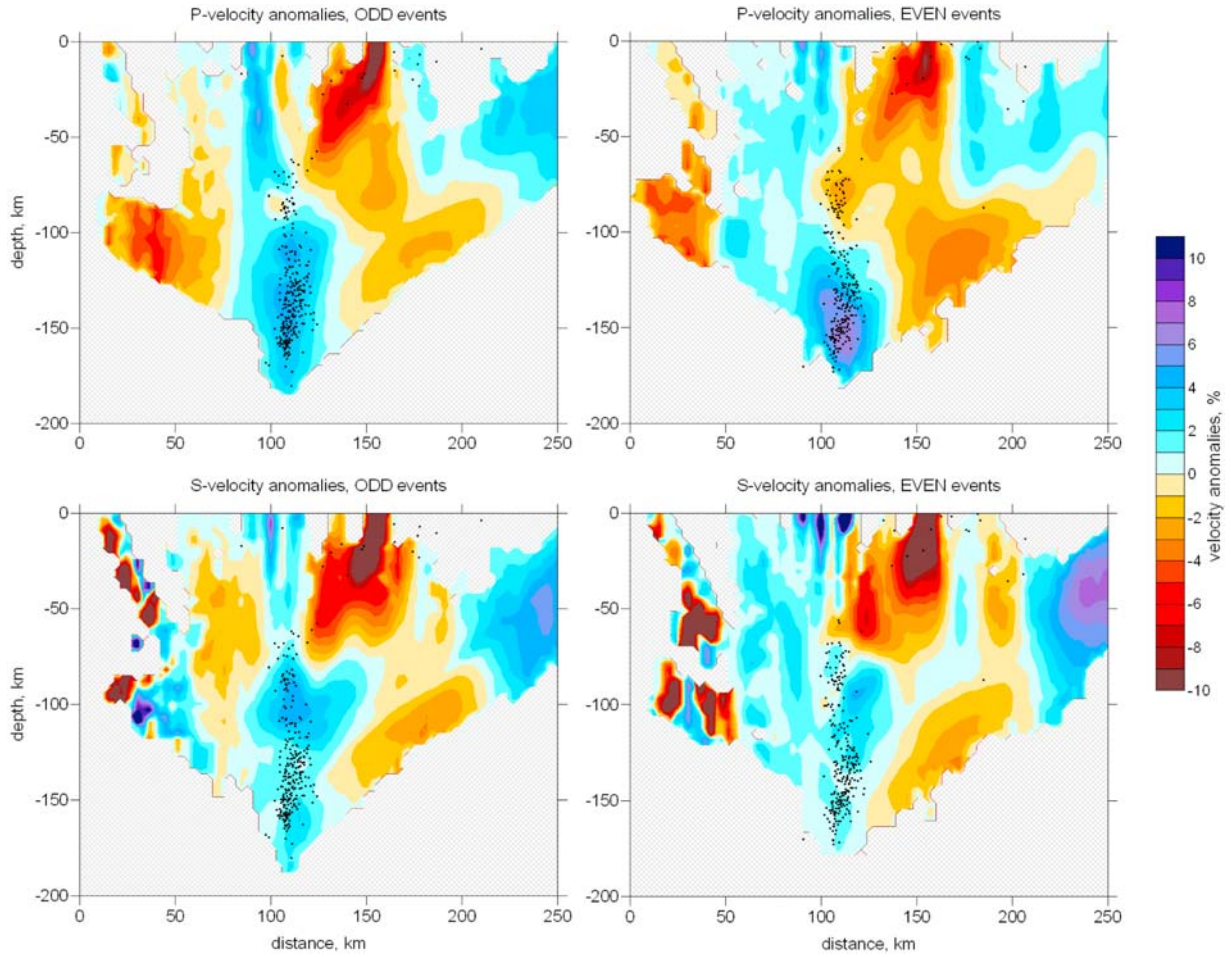

Figure C2. Same as Figure C1 but presented in a vertical section. Location of the section is indicated in Figure C1.

inversion. For example, defining the synthetic patterns in the same parameterization nodes/blocks used for inversion is not appropriate as it fixes the periodicity of anomalies in the most convenient way for the algorithm. In reality, such predefinition of structural periodicity is, of course, not available.

[49] 2. The concept of the optimal 1-D model used for computing synthetic times should be substituted with a more realistic acceptance of starting from an approximated 1-D model. It was showed that in terms of relative variation of velocity, the results are not affected by this choice [*Koulakov*, 2009].

[50] 3. After computing the synthetic travel times, the coordinates and origin times of sources should not be used in the inversion procedure. In fact, ideally, the synthetic data file should not contain any information about the sources, and their location should begin from the initial stage. However, one can also begin the inversion procedure using the rough source locations in the 1-D velocity model because they are generally different from the "true" 3-D locations, thus respecting the rule.

[51] 4. When reconstructing the synthetic model, all parameters and procedural steps should be absolutely identical to observed data processing.

[52] The synthetic testing performed according to these rules allows not only the assessment of the resolution of the model, but also estimation of optimal values of the free inversion parameters (e.g., amplitude damping and smoothing), which can be then used to enhance the real data results. For this study, we inverted synthetic and observed data in turn several times to obtain the best values for the parameters.

[53] The synthetic travel times are computed by bending ray tracing through the synthetic model,

Figure C1. Odd-even test. Results for two halved subsets are presented for P and S anomalies in three horizontal sections. Dots depict the relocated sources around the sections.

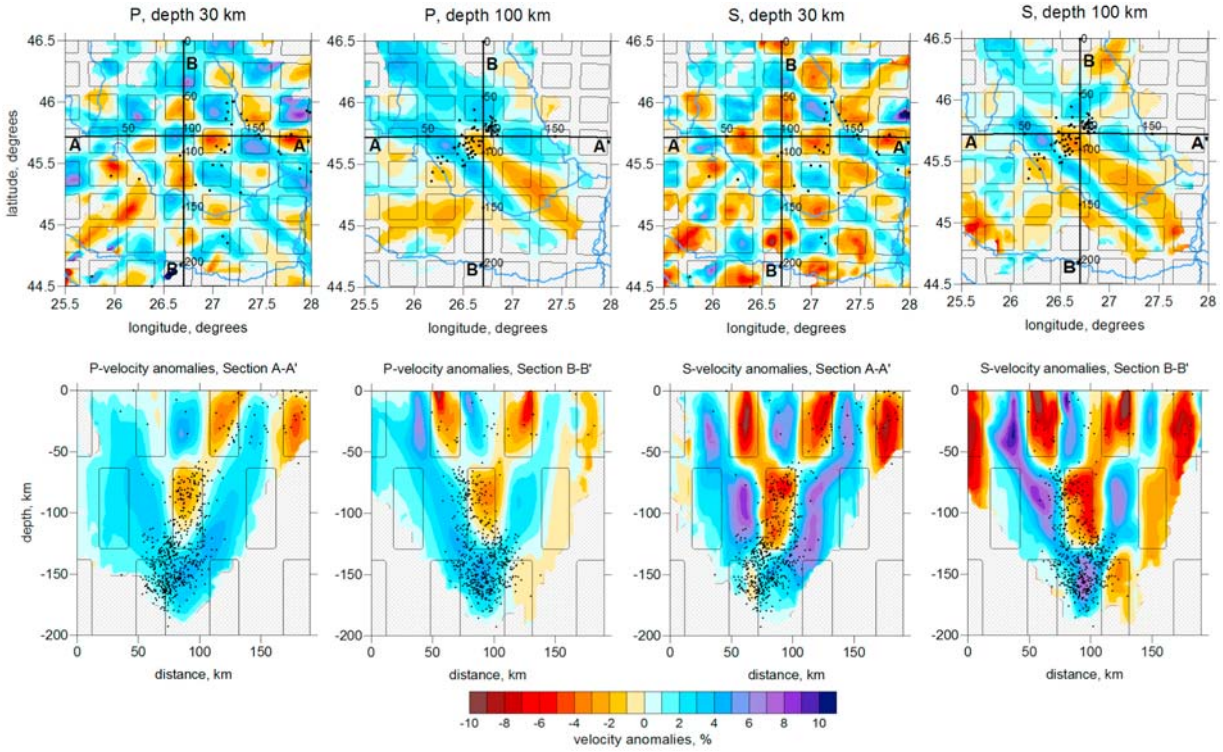

Figure D1. Checkerboard test performed according to Vp-Vs scheme in (top) two horizontal sections and (bottom) two vertical sections. Initial synthetic patterns are highlighted with thin black lines. Locations of the profiles are indicated in all maps. Relocated sources are shown with black dots.

which is represented by alternating positive and negative velocity anomalies summed up with the 1-D velocity model indicated in Figure 4c by a red line. Laterally, the size of the patterns is 30 km along the latitude and longitude. In the vertical direction the change of sign is defined at 65 km and 140 km depth. The configuration of the model is shown in Figure D1 with thin black lines in map view and in vertical sections. The amplitudes of the anomalies were ±5% and ±7% for P and S models, respectively. The computed synthetic times were perturbed with random noise that have a realistic distribution histogram constructed previously from analyses of many different actual data sets. This histogram is slightly biased with respect to the traditionally used normal Gaussian distribution. The average amplitude of noise was defined at 0.1 s and 0.15 s for P and S synthetic travel time data, respectively.

[54] The reconstruction begins with the relocation of the sources and the optimization of the 1-D velocity model. We have performed the reconstructions with two starting models, which are indicated in Figure 4c by violet and green lines. Here, we present the result that corresponds to the violet lines; however, for the other case, the obtained anomalies are identical. This shows again that the tomography inversion for this observation scheme provides the relative anomalies more robustly than absolute velocities, which should be interpreted carefully. The results of reconstructed P and S anomalies in the checkerboard tests are shown in Figure D1 in map view at depths between 30 and 110 km and in two vertical sections. It can be seen that in the upper section the periodic anomalies are reconstructed in most parts of the study area, while for the deeper layers the anomalies are reconstructed only in the central part where earthquakes occur. We detect some diagonal smearing that should be taken into account when real data results are interpreted. In vertical sections, both P and S models demonstrate a rather robust reconstruction of the level at 65 km where checkerboard anomalies change sign. This seems to be important for considering the real data results where a change of sign also takes place at this depth.

Appendix E: Reconstruction of Realistic Patterns

[55] The result of seismic tomography inversion is like a photograph taken by a camera with a blurred

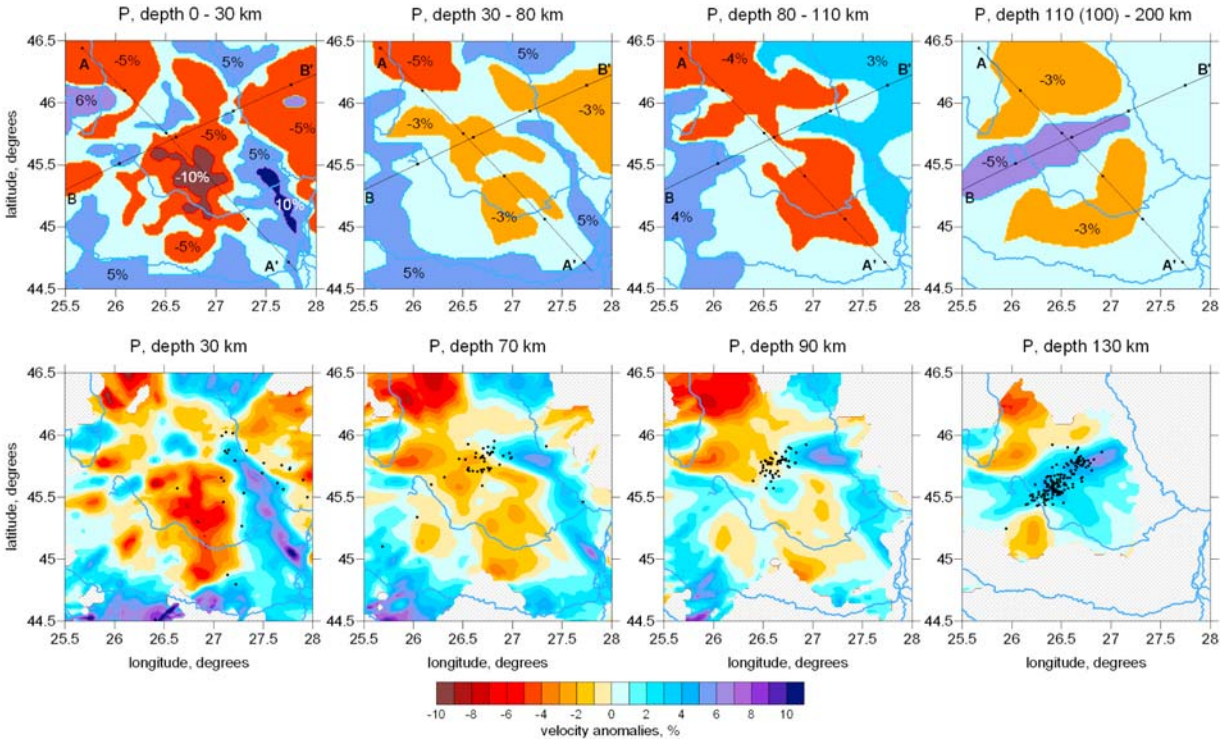

Figure E1. Synthetic test aimed at reproducing the results of the real experiment. Only results for P velocity modeling are shown in horizontal sections. (top) Synthetic model defined in 3-D prisms. Values of anomalies are indicated by nu anomalies; depth diapason of prism definition is given above each plot. (bottom) Reconstruction results for P velocity anomalies and source locations (black dots).

and deformed lens, which biases the shapes and "colors" (amplitudes) of the true images. Therefore, it appears to be inadequate to report the quantitative parameters obtained after inversion of observed data as real data. We propose a test that allows for the investigation of the properties of the "camera" (inversion algorithm) and to retrieve information about probabilistic shapes and amplitudes of velocity anomalies on Earth. Furthermore, this test allows us to find the optimal values of free parameters (e.g., damping) used for inversion.

[56] The purpose of this test is to build a synthetic model, which, after performing forward and inverse modeling, reproduces similar patterns as in the case of observed data inversion. Note that the inverse procedure (tomography + source location) should be performed absolutely identically and with the same free parameters as in the case of observed data. The initial locations of sources and "true" reference model should be "forgotten." Furthermore, after computing synthetic travel times, a random noise should be added, and its level is defined to provide the similar variance reduction, as in reality. When the inversion resembles the retrieved models in both the real and synthetic cases, the synthetic model may adequately reflect the structures on the real Earth. However, we admit that this procedure is theoretically nonunique and several models may lead to similar reconstructions. For example, such nonuniqueness due to vertical smearing was shown with two models for the Toba area, N. Sumatra [*Koulakov et al.*, 2009]. This modeling allows us to investigate this effect and take it into account.

[57] The synthetic model with realistic patterns for P wave velocity anomalies is shown in horizontal and vertical sections in Figures E1 and E2. For the S model, the shape of patterns remained the same, but the amplitudes were 20–30% higher. The anomalies are defined in prisms that may have a complex shape when seen in map view and remain unchanged within a fixed depth interval. The prisms are defined in the depth ranges indicated in Figure E1, except for one deep high-velocity anomaly, which is defined from 100 to 200 km. We performed several trials testing the, shapes and amplitudes of the synthetic patterns. The final model, which is presented in Figures E1 and E2,

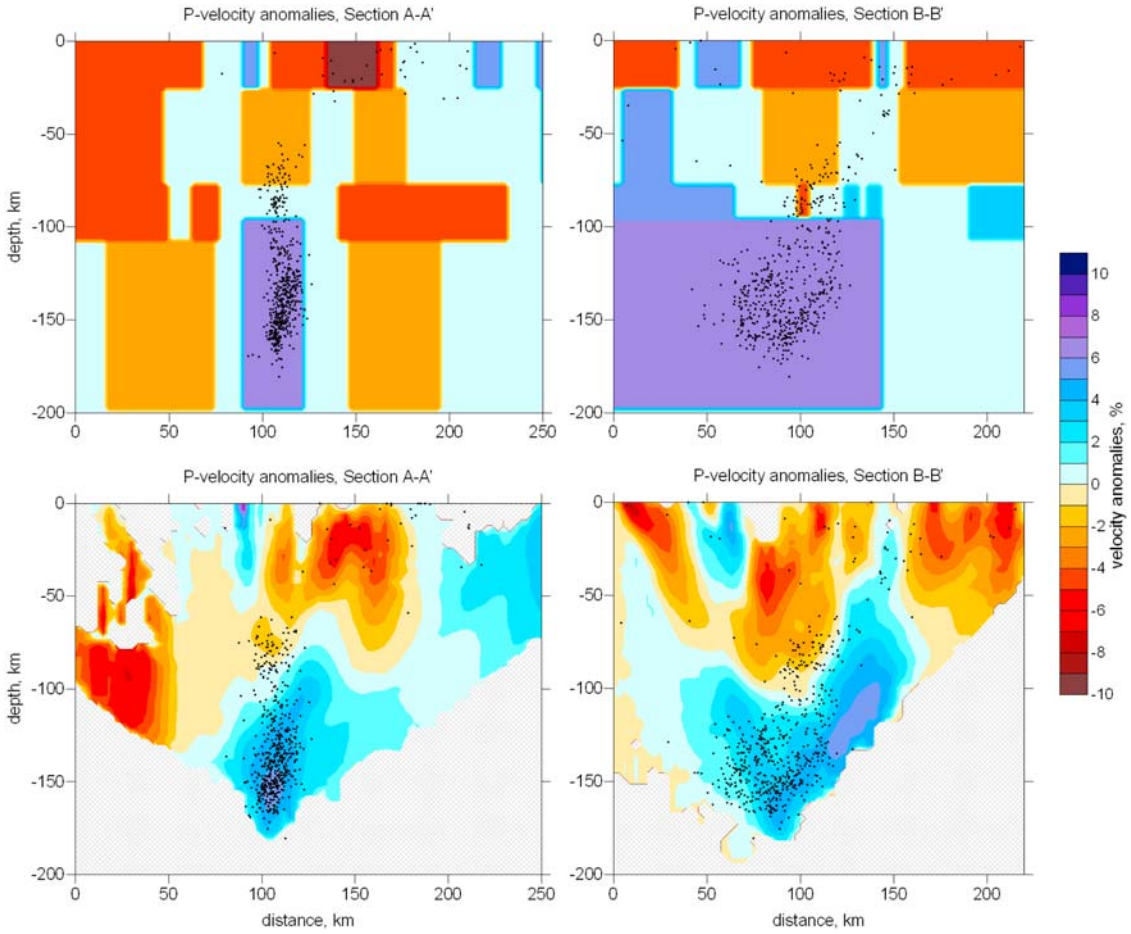

Figure E2. Same test as in Figure E1 but shown in two vertical sections A–A′ and B–B′ with locations indicated in Figure E1 (top). (top) P synthetic model and (bottom) the reconstruction results for P velocity anomalies and source locations (black dots).

is quite similar to the actual anomalies shown in Figures 5 and 7.

Acknowledgments

[58] The earthquake data are provided by the CALIXTO'99 experiment and K2 network within the CRC461 program of University of Karlsruhe (Germany) and the Romanian Seismic Network. The work of Ivan Koulakov is supported by the Russian Federation for Basic Researches (08-05-00276-a), Helmholtz Society and RFBR Joint Research Project 09-05-91321-SIG a, multidisciplinary projects SB RAS 21 and SB-UrO-DVORAS 96, and project ONZ RAS 7.4. The training stages of Bogdan Zaharia at German Research Centre for Geosciences, Potsdam, Germany were funded by the CORINT project 49/2006 of the Romania Ministry of Education and Research and NATO SfP project 981881. We are grateful to the Editor, Thorsten Becker, for rigorous and constructive criticism, as well as to Lapo Boschi and an anonymous reviewer for their critical remarks which helped us to improve the paper.

References

Babeyko, A. Y., S. V. Sobolev, T. Vietor, R. B. Trumbull, and O. Oncken (2006), Weakening of the upper plate during tectonic shortening: Thermo-mechanical causes and consequences, in *Frontiers in Earth Sciences*, vol. 1, *The Andes: Active Subduction Orogeny*, edited by O. Oncken et al., pp. 495–512, Springer, Berlin.

Badescu, D. (2005), *The Evolution of the Tectono-Stratigraphy of the Eastern Carpathians During Mesozoic and Neogene Times* (in Romanian), 308 pp., Ed. Econ., Bucharest.

Bird, P. (1979), Continental delamination and the Colorado Plateau, *J. Geophys. Res.*, *84*, 7561–7571.

Bonjer, K.-P., and M. Rizescu (2000), Data release 1996–1999 of the Vrancea K2 Seismic Network [CD-ROM], Natl. Inst. for Earth Phys., Magurele, 15 July.

Bonjer, K.-P., M. C. Oncescu, M. Rizescu, D. Enescu, L. Driad, M. Radulian, C. Ionescu, and T. Moldoveanu (2000), Source- and site-parameters of the April 28, 1999 intermediate depth Vrancea earthquake: First results from the new K2 network in Romania, paper presented at XXVII General Assembly, Eur. Seismol. Comm., Lisbon, Portugal.

Bonjer, K.-P., M. Rizescu, and B. Grecu (2002), Data release 2000–2001 of the Vrancea K2 Seismic Network [CD-ROM], Natl. Inst. for Earth Phys., Magurele, 24 Oct.

Boschi, L., B. Fry, G. Ekström, and D. Giardini (2009), The Mediterranean upper mantle as seen by surface waves, *Surv. Geophys.*, *30*, 463–501, doi:10.1007/s10712-009-9066-2.

Buiter, S. J. H., R. Govers, and M. J. R. Wortel (2002), Two-dimensional simulations of surface deformations caused by slab detachment, *Tectonophysics*, *354*, 195–210, doi:10.1016/S0040-1951(02)00336-0.

Burchfiel, B. C. (1976), *Geology of Romania*, *Spec. Pap. Geol. Soc. Am.*, *158*, 82 pp.

Constantinescu, L., and D. Enescu (1984), A tentative approach to possibly explaining the occurrence of the Vrancea earthquakes, *Rev. Roum. Geol. Geophys. Geogr. Geophys.*, *28*, 19–32.

Csontos, L. (1995), Tertiary tectonic evolution of the Intra-Carpathian area: A review, *Acta Vulcanol.*, *7*(2), 1–13.

Csontos, L., and A. Voros (2004), Mesozoic plate tectonic reconstruction of the Carpathian region, *Palaeogeogr. Palaeoclimatol. Palaeoecol.*, *210*, 1–56, doi:10.1016/j.palaeo.2004.02.033.

Ducea, M. N., and J. B. Saleeby (1998), A case for delamination of the deep batholithic crust beneath the Sierra Nevada, California, *Int. Geol. Rev.*, *40*(1), 78–93, doi:10.1080/00206819809465199.

Ellouz, N., and E. Roca (1994), Palinspastic reconstructions of the Carpathians and adjacent areas since the Cretaceous: A quantitative approach, in *Peri-Tethyan Platforms*, edited by F. Roure, pp. 51–78, Technip, Paris.

Enescu, D., and B. D. Enescu (1998), Seismotectonic model regarding the genesis and the occurrence of Vrancea (Romania) earthquakes, *Rom. Rep. Phys.*, *50*(1–2), 97–122.

Enescu, D., I. Cornea, F. Radulescu, V. Raileanu, and A. Pompilian (1982), Seismological data on deep structure of Vrancea region, *Rev. Roum. Geol. Geophys. Geogr. Geophys.*, *26*, 29–36.

Fan, G., T. C. Wallace, and D. Zhao (1998), Tomographic imaging of deep velocity structure beneath the eastern and southern Carpathians, Romania: Implications for continental collision, *J. Geophys. Res.*, *103*, 2705–2724, doi:10.1029/97JB01511.

Fuchs, K., et al. (1979), The Romanian earthquake of March 4, 1979. II. Aftershocks and migration of seismic activity, *Tectonophysics*, *53*, 225–247, doi:10.1016/0040-1951(79)90068-4.

Gilbert, H., C. Jones, T. J. Owens, and G. Zandt (2007), Imaging Sierra Nevada lithosphere sinking, *Eos Trans. AGU*, *88*(21), 225–229, doi:10.1029/2007EO210001.

Houseman, G. A., and P. Molnar (1997), Gravitational (Rayleigh-Taylor) instability of a layer with non-linear viscosity and convective thinning of continental lithosphere, *Geophys. J. Int.*, *128*, 125–150, doi:10.1111/j.1365-246X.1997.tb04075.x.

Kay, R. W., and S. M. Kay (1993), Delamination and delamination magmatism, *Tectonophysics*, *219*, 177–189, doi:10.1016/0040-1951(93)90295-U.

Kissling, E., W. L. Ellworth, D. Eberhart-Phillips, and U. Kradolfer (1994), Initial reference models in local earthquake tomography, *J. Geophys. Res.*, *99*, 19,635–19,646.

Knapp, J. H., C. C. Knapp, V. Raileanu, L. Matenco, V. Mocanu, and C. Dinu (2005), Crustal constraints on the origin of mantle seismicity in the Vrancea Zone, Romania: The case for active continental lithospheric delamination, *Tectonophysics*, *410*, 311–323, doi:10.1016/j.tecto.2005.02.020.

Koch, M. (1985), Nonlinear inversion of local seismic travel times for the simultaneous determination of the 3D-velocity structure and hypocenters—Application to the seismic zone Vrancea, *J. Geophys.*, *56*, 160–173.

Koulakov, I. (2009), LOTOS code for local earthquake tomographic inversion. Benchmarks for testing tomographic algorithms, *Bull. Seismol. Soc. Am.*, *99*(1), 194–214, doi:10.1785/0120080013.

Koulakov, I., and S. Sobolev (2006a), Moho depth and three-dimensional P and S structure of the crust and uppermost mantle in the eastern Mediterranean and Middle East derived from tomographic inversion of local ISC data, *Geophys. J. Int.*, *164*(1), 218–235, doi:10.1111/j.1365-246X.2005.02791.x.

Koulakov, I., and S. V. Sobolev (2006b), A tomographic image of Indian lithosphere break-off beneath the Pamir Hindukush Region, *Geophys. J. Int.*, *164*, 425–440, doi:10.1111/j.1365-246X.2005.02841.x.

Koulakov, I., et al. (2007), P and S velocity structure of the crust and the upper mantle beneath central Java from local tomography inversion, *J. Geophys. Res.*, *112*, B08310, doi:10.1029/2006JB004712.

Koulakov, I., T. Yudistira, B.-G. Luehr, and Wandono (2009), *P*, *S* velocity and V_P/V_S ratio beneath the Toba caldera complex (northern Sumatra) from local earthquake tomography, *Geophys. J. Int.*, *177*, 1121–1139, doi:10.1111/j.1365-246X.2009.04114.x.

Lankreijer, A., V. Mocanu, and S. A. P. L. Cloetingh (1997), Lateral variations in lithosphere strength in the Romanian Carpathians: Constraints on basin evolution, *Tectonophysics*, *272*, 269–290, doi:10.1016/S0040-1951(96)00262-4.

Linzer, H. G., W. Frisch, P. Zweigel, R. Girbacea, H. P. Hann, and F. Moser (1998), Kinematic evolution of the Romanian Carpathians, *Tectonophysics*, *297*, 133–156, doi:10.1016/S0040-1951(98)00166-8.

Lorenz, F. P., M. Martin, B. Sperner, F. Wenzel, and M. Popa (1997), Teleseismic travel-time tomography of the compressional-wave velocity structure in the Vrancea zone, Romania, *Eos Trans. AGU*, *78*(46), Fall Meet. Suppl., F497.

Lorinczi, P., and G. A. Houseman (2009), Lithospheric gravitational instability beneath the southeast Carpathians, *Tectonophysics*, *474*(1–2), 322–336, doi:10.1016/j.tecto.2008.05.024.

Martin, M., J. R. R. Ritter, and the CALIXTO Working Group (2005), High-resolution teleseismic body-wave tomography beneath SE Romania—I. Implications for three-dimensional versus one-dimensional crustal correction strategies with a new crustal velocity model, *Geophys. J. Int.*, *162*(2), 448–460, doi:10.1111/j.1365-246X.2005.02661.x.

Martin, M., F. Wenzel, and the CALIXTO Working Group (2006), High-resolution teleseismic body wave tomography beneath SE-Romania—II. Imaging of a slab detachment scenario, *Geophys. J. Int.*, *164*, 579–595, doi:10.1111/j.1365-246X.2006.02884.x.

Mason, P. R. D., I. Seghedi, A. Szakacs, and H. Downes (1998), Magmatic constraints on geodynamic models of subduction in the East Carpathians, Romania, *Tectonophysics*, *297*, 157–176, doi:10.1016/S0040-1951(98)00167-X.

Matenco, L., R. Zoetemeijer, S. Cloetingh, and C. Dinu (1997), Lateral variations in mechanical properties of the Romanian external Carpathians: Inferences of flexure and gravity modeling, *Tectonophysics*, *282*, 147–166, doi:10.1016/S0040-1951(97)00217-5.

McKenzie, D. (1970), Active tectonics of the Mediterranean region, *Nature*, *226*, 239–243.

Nakajima, J., T. Matsuzawa, A. Hasegawa, and D. Zhao (2001), Three-dimensional structure of Vp, Vs, and Vp/Vs

beneath northeastern Japan: Implications for arc magmatism and fluids, *J. Geophys. Res.*, *106*, 21,843–21,857.

Neagoe, C., and C. Ionescu (2009), Toward a dense real-time seismic network in Romania, *Rom. Rep. Phys.*, *61*(2), 359–366.

Nelson, K. D. (1991), A unified view of craton evolution motivated by recent deep seismic reflection and refraction results, *Geophys. J. Int.*, *105*(1), 25–35, doi:10.1111/j.1365-246X.1991.tb03441.x.

Oncescu, M. C. (1982), Velocity structure of the Vrancea region, Romania, *Tectonophysics*, *90*, 117–122, doi:10.1016/0040-1951(82)90256-6.

Oncescu, M. C. (1984), Deep structure of Vrancea region, Romania, inferred from simultaneous inversion for hypocenters and 3-D velocity structure, *Ann. Geophys.*, *2*, 23–28.

Oncescu, M. C., V. Burlacu, M. Anghel, and V. Smalbergher (1984), Three dimensional P wave velocity image under the Carpathian Arc, *Tectonophysics*, *106*, 305–319, doi:10.1016/0040-1951(84)90182-3.

Oncescu, M. C., M. Rizescu, and K. P. Bonjer (1996), SAPS—A completely automated and networked seismological acquisition and processing system, *Comput. Geosci.*, *22*, 89–97, doi:10.1016/0098-3004(95)00060-7.

Oncescu, M. C., V. Marza, M. Rizescu, and M. Popa (1999), The Romanian earthquakes catalogue between 984–1997, in *Vrancea Earthquakes: Tectonics, Hazard and Risk Mitigation*, edited by F. Wenzel and D. Lungu, pp. 43–47, Kluwer Acad., Dordrecht, Netherlands.

Paige, C. C., and M. A. Saunders (1982), LSQR: An algorithm for sparse linear equations and sparse least squares, *Trans. Math. Software*, *8*, 43–71, doi:10.1145/355984.355989.

Pecskay, Z., O. Edelstein, I. Seghedi, A. Szakacs, M. Kovacs, M. Crihan, and M. Bernad (1995), K-Ar datings of Neogene-Quaternary calc-alkaline volcanic rocks in Romania, *Acta Vulcanol.*, *7*, 53–62.

Popa, M., E. Kissling, M. Radulian, K. P. Bonjer, D. Enescu, S. Dragan, and the CALIXTO Working Group (2001), Local source tomography using body waves to deduce a minimum 1D velocity model for the Vrancea (Romania) zone, *Rom. Rep. Phys.*, *53*, 519–536.

Popa, M., M. Radulian, B. Grecu, E. Popescu, and A. O. Placinta (2005), Attenuation in south-eastern Carpathians area: Result of upper mantle inhomogeneity, *Tectonophysics*, *410*, 235–249, doi:10.1016/j.tecto.2004.12.037.

Radulian, M., and M. Popa (1996), Scaling of the source parameters for the Vrancea intermediate depth earthquakes, *Tectonophysics*, *261*, 67–81, doi:10.1016/0040-1951(96)00057-1.

Radulian, M., M. Popa, O. F. Cărbunar, and M. Rogozea (2008), Seismicity patterns in Vrancea and predictive features, *Acta Geod. Geophys. Hung.*, *43*, 163–173, doi:10.1556/AGeod.43.2008.2-3.6.

Ratschbacher, L., O. Merle, P. Davy, and P. Cobbold (1991), Lateral extrusion in the Eastern Alps, part I: Boundary conditions and experiments scaled for gravity, *Tectonics*, *10*, 245–256, doi:10.1029/90TC02622.

Roca, E., G. Bessereau, E. Jawor, M. Kotarba, and F. Roure (1995), Pre-Neogene evolution of the Western Carpathians: Constraints from the Bochnia-Tatra Mountains section (Polish Western Carpathians), *Tectonics*, *14*(4), 855–873, doi:10.1029/95TC00828.

Roure, F., E. Roca, and W. Sassi (1993), The Neogene evolution of the outer Carpathian flysch units (Poland, Ukraine and Romania): Kinematics of a foreland, *Sediment. Geol.*, *86*, 177–201, doi:10.1016/0037-0738(93)90139-V.

Russo, R. M., V. Mocanu, M. Radulian, M. Popa, and K.-P. Bonjer (2005), Seismic attenuation in the Carpathian bend zone and surroundings, *Earth Planet. Sci. Lett.*, *237*, 695–709, doi:10.1016/j.epsl.2005.06.046.

Seber, D., M. Barazangi, A. Ibenbrahim, and A. Demnati (1996), Geophysical evidence for lithospheric delamination beneath the Alboran Sea and Rif–Betic mountains, *Nature*, *379*, 785–790, doi:10.1038/379785a0.

Seghedi, I., H. Downes, A. Szakacs, P. R. D. Mason, M. F. Thirlwall, E. Rosu, Z. Pecskay, E. Marton, and C. Panaiotu (2004), Neogene-Quaternary magmatism and geodynamics in the Carpathian-Pannonian region: A synthesis, *Lithos*, *72*, 117–146, doi:10.1016/j.lithos.2003.08.006.

Sobolev, S. V., A. Y. Babeyko, I. Koulakov, and O. Oncken (2006), Mechanism of the Andean orogeny: Insight from the numerical modeling, in *Frontiers in Earth Sciences*, vol. 1, *The Andes: Active Subduction Orogeny*, edited by O. Oncken et al., pp. 513–535, Springer, Berlin.

Sperner, B., F. Lorenz, K. Bonjer, S. Hettel, B. Muller, and F. Wenzel (2001), Slab break-off—Abrupt cut or gradual detachment? New insights from the Vrancea region (SE Carpathians, Romania), *Terra Nova*, *13*(3), 172–179, doi:10.1046/j.1365-3121.2001.00335.x.

Van der Sluis, A., and H. A. van der Vorst (1987), Numerical solution of large, sparse linear algebraic systems arising from tomographic problems, in *Seismic Tomography*, edited by G. Nolet, pp. 49–83, D. Reidel, Dordrecht, Netherlands.

van de Zedde, D. M. A., and M. J. R. Wortel (2001), Shallow slab detachment as a transient source of heat at midlithospheric depths, *Tectonics*, *20*, 868–882, doi:10.1029/2001TC900018.

Wenzel, F., U. Achauer, D. Enescu, E. Kissling, R. Russo, V. Mocanu, and G. Mussachio (1998), The final stage of plate detachment: International tomographic experiment in Romania aims to a high-resolution snapshot of this process, *Eos Trans. AGU*, *79*(589), 592–594.

Wenzel, F., F. P. Lorentz, B. Sperner, and M. Oncescu (1999), Seismotectonics of the Romanian Vrancea area, in *Vrancea Earthquakes: Tectonics, Hazard and Risk Mitigation*, edited by F. Wenzel, O. Novak, and D. Lungu, pp. 15–25, Kluwer Acad., Dordrecht, Netherlands.

Wortel, M. J. R., and W. Spakman (1992), Structure and dynamics of subducted lithosphere in the Mediterranean region, *Proc. K. Ned. Akad. Wet.*, *95*, 325–347.

Wortel, M. J. R., and W. Spakman (1993), The dynamic evolution of the Apenninic-Calabrian, Hellenic and Carpathian arcs: A unifying approach, *Terra Nova*, *5*, suppl., 97.

Wortel, R., and W. Spakman (2000), Subduction and slab detachment in the Mediterranean–Carpathian region, *Science*, *290*, 1910–1917, doi:10.1126/science.290.5498.1910.